(12) INTERNATIONAL APPLICATION PUBLISHED UNDER THE PATENT COOPERATION TREATY (PCT)

(19) World Intellectual Property Organization
International Bureau

(43) International Publication Date
14 October 2010 (14.10.2010)

PCT

(10) International Publication Number
WO 2010/118401 A2

(51) International Patent Classification:
A63B 37/14 (2006.01) *A63B 37/12* (2006.01)

(21) International Application Number:
PCT/US2010/030646

(22) International Filing Date:
9 April 2010 (09.04.2010)

(25) Filing Language: English

(26) Publication Language: English

(30) Priority Data:
61/168,134 9 April 2009 (09.04.2009) US

(71) Applicant *(for all designated States except US)*: **AERO-X GOLF INC.** [—/US]; 20844 Wild Willow Hollow, Escondido, California 92029 (US).

(72) Inventors; and
(75) Inventors/Applicants *(for US only)*: **FELKER, David L.** [US/US]; 20844 Wild Willow Hollow, Escondido, California 92029 (US). **WINFIELD, Douglas C.** [US/US]; 1 Carriage Hill, Madison, Alabama 35758 (US). **LEE, Rocky** [CA/US]; 2001 Hamilton Street #1429, Philadephia, Pennsylvania 19130 (US).

(74) Agents: **GILLESPIE, Noel, C.** et al.; Procopio, Cory, Hargreaves & Savitch LLP, 525 B Street, Suite 2200, San Diego, California 92101 (US).

(81) Designated States *(unless otherwise indicated, for every kind of national protection available)*: AE, AG, AL, AM, AO, AT, AU, AZ, BA, BB, BG, BH, BR, BW, BY, BZ, CA, CH, CL, CN, CO, CR, CU, CZ, DE, DK, DM, DO, DZ, EC, EE, EG, ES, FI, GB, GD, GE, GH, GM, GT, HN, HR, HU, ID, IL, IN, IS, JP, KE, KG, KM, KN, KP, KR, KZ, LA, LC, LK, LR, LS, LT, LU, LY, MA, MD, ME, MG, MK, MN, MW, MX, MY, MZ, NA, NG, NI, NO, NZ, OM, PE, PG, PH, PL, PT, RO, RS, RU, SC, SD, SE, SG, SK, SL, SM, ST, SV, SY, TH, TJ, TM, TN, TR, TT, TZ, UA, UG, US, UZ, VC, VN, ZA, ZM, ZW.

(84) Designated States *(unless otherwise indicated, for every kind of regional protection available)*: ARIPO (BW, GH,

[Continued on next page]

(54) Title: A LOW LIFT GOLF BALL

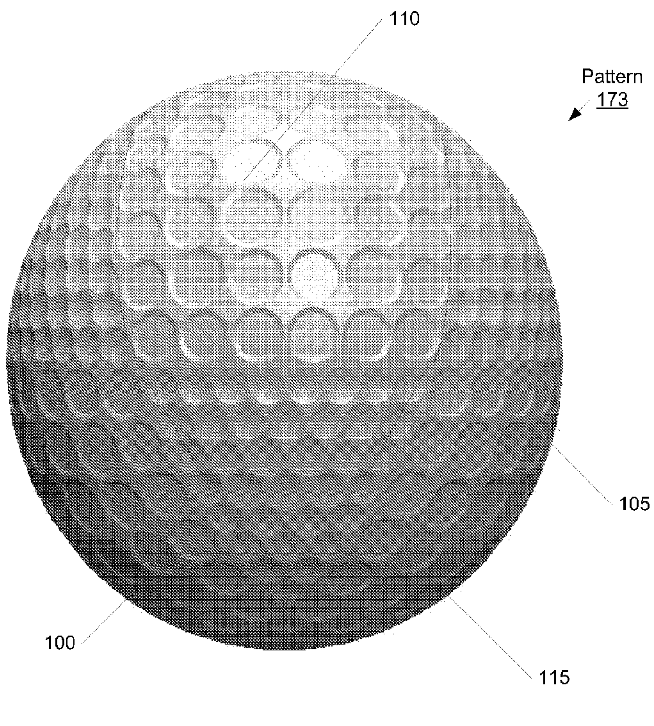

FIG. 2

(57) Abstract: A golf ball having a plurality of dimples formed on its outer surface, the outer surface of the golf ball being divided into first and second areas each containing a plurality of dimples, the first and second areas being of different shapes, each first area containing first dimples and each second area containing second dimples, at least some first dimples being of different types from the second dimples, and the first areas being formed of circular paths around the outer surface of the ball, the second areas being formed by the intersection of the circular paths.

WO 2010/118401 A2

GM, KE, LR, LS, MW, MZ, NA, SD, SL, SZ, TZ, UG, ZM, ZW), Eurasian (AM, AZ, BY, KG, KZ, MD, RU, TJ, TM), European (AT, BE, BG, CH, CY, CZ, DE, DK, EE, ES, FI, FR, GB, GR, HR, HU, IE, IS, IT, LT, LU, LV, MC, MK, MT, NL, NO, PL, PT, RO, SE, SI, SK, SM, TR), OAPI (BF, BJ, CF, CG, CI, CM, GA, GN, GQ, GW, ML, MR, NE, SN, TD, TG).

Published:

— *without international search report and to be republished upon receipt of that report (Rule 48.2(g))*

SPECIFICATION

A LOW LIFT GOLF BALL

BACKGROUND

1. Technical Field

[0001] The embodiments described herein are related to the field of golf balls and, more particularly, to a spherically symmetrical golf ball having a dimple pattern that generates low-lift in order to control dispersion of the golf ball during flight.

2. Related Art

[0002] The flight path of a golf ball is determined by many factors. Several of the factors can be controlled to some extent by the golfer, such as the ball's velocity, launch angle, spin rate, and spin axis. Other factors are controlled by the design of the ball, including the ball's weight, size, materials of construction, and aerodynamic properties.

[0003] The aerodynamic force acting on a golf ball during flight can be broken down into three separate force vectors: Lift, Drag, and Gravity. The lift force vector acts in the direction determined by the cross product of the spin vector and the velocity vector. The drag force vector acts in the direction opposite of the velocity vector. More specifically, the aerodynamic properties of a golf ball are characterized by its lift and drag coefficients as a function of the Reynolds Number (Re) and the Dimensionless Spin Parameter (DSP). The Reynolds Number is a dimensionless quantity that quantifies the ratio of the inertial to viscous forces acting on the golf ball as it flies through the air. The Dimensionless Spin Parameter is the ratio of the golf ball's rotational surface speed to its speed through the air.

[0004] Since the 1990's, in order to achieve greater distances, a lot of golf ball development has been directed toward developing golf balls that exhibit improved distance through lower drag under conditions that would apply to, e.g., a driver shot immediately after club impact as well as relatively high lift under conditions that would apply to the latter portion of, e.g., a driver shot as the ball is descending towards the ground. A lot of this development was enabled by new measurement devices that could more accurately and efficiently measure golf ball spin, launch angle, and velocity immediately after club impact.

[0005] Today the lift and drag coefficients of a golf ball can be measured using several different methods including an Indoor Test Range such as the one at the USGA Test Center in Far Hills, New Jersey, or an outdoor system such as the Trackman Net System made by Interactive Sports Group in Denmark. The testing, measurements, and reporting of lift and drag coefficients for conventional golf balls has generally focused on the golf ball spin and velocity conditions for a well hit straight driver shot - approximately 3,000 rpm or less and an initial ball velocity that results from a driver club head velocity of approximately 80-100 mph.

[0006] For right-handed golfers, particularly higher handicap golfers, a major problem is the tendency to "slice" the ball. The unintended slice shot penalizes the golfer in two ways: 1) it causes the ball to deviate to the right of the intended flight path and 2) it can reduce the overall shot distance.

[0007] A sliced golf ball moves to the right because the ball's spin axis is tilted to the right. The lift force by definition is orthogonal to the spin axis and thus for a sliced golf ball the lift force is pointed to the right.

[0008] The spin-axis of a golf ball is the axis about which the ball spins and is usually orthogonal to the direction that the golf ball takes in flight. If a golf ball's spin axis is 0 degrees, i.e., a horizontal spin axis causing pure backspin, the ball will not hook or slice and a higher lift force combined with a 0-degree spin axis will only make the ball fly higher. However, when a ball is hit in such a way as to impart a spin axis that is more than 0 degrees, it hooks, and it slices with a spin axis that is less than 0 degrees. It is the tilt of the spin axis that directs the lift force in the left or right direction, causing the ball to hook or slice. The distance the ball unintentionally flies to the right or left is called Carry Dispersion. A lower flying golf ball, i.e., having a lower lift, is a strong indicator of a ball that will have lower Carry Dispersion.

[0009] The amount of lift force directed in the hook or slice direction is equal to: Lift Force * Sine (spin axis angle). The amount of lift force directed towards achieving height is: Lift Force * Cosine (spin axis angle).

[0010] A common cause of a sliced shot is the striking of the ball with an open clubface. In this case, the opening of the clubface also increases the effective loft of the club and thus increases the total spin of the ball. With all other factors held constant, a higher ball spin rate will in general produce a higher lift force and this is why a slice shot will often have a higher trajectory than a straight or hook shot.

[0011] Table 1 shows the total ball spin rates generated by a golfer with club head speeds ranging from approximately 85-105 mph using a 10.5 degree driver and hitting a variety of prototype golf balls and commercially available golf balls that are considered to be low and normal spin golf balls:

Spin Axis, degree	Typical Total Spin, rpm	Type Shot
-30	2,500 - 5,000	Strong Slice
-15	1,700 – 5,000	Slice
0	1,400 – 2,800	Straight
+15	1,200 – 2,500	Hook
+30	1,000 – 1,800	Strong Hook

TABLE 1

[0012] If the club path at the point of impact is "outside-in" and the clubface is square to the target, a slice shot will still result, but the total spin rate will be generally lower than a slice shot hit with the open clubface. In general, the total ball spin will increase as the club head velocity increases.

[0013] In order to overcome the drawbacks of a slice, some golf ball manufacturers have modified how they construct a golf ball, mostly in ways that tend to lower the ball's spin rate. Some of these modifications include: 1) using a hard cover material on a two-piece golf ball, 2) constructing multi-piece balls with hard boundary layers and relatively soft thin covers in order to lower driver spin rate and preserve high spin rates on short irons, 3) moving more weight towards the outer layers of the golf ball thereby increasing the moment of inertia of the golf ball, and 4) using a cover that is constructed or treated in such a ways so as to have a more slippery surface.

[0014] Others have tried to overcome the drawbacks of a slice shot by creating golf balls where the weight is distributed inside the ball in such a way as to create a preferred axis of rotation.

[0015] Still others have resorted to creating asymmetric dimple patterns in order to affect the flight of the golf ball and reduce the drawbacks of a slice shot. One such example was the Polara™ golf ball with its dimple pattern that was designed with different type dimples in the polar and equatorial regions of the ball.

[0016] In reaction to the introduction of the Polara golf ball, which was intentionally manufactured with an asymmetric dimple pattern, the USGA created the "Symmetry Rule". As a result, all golf balls not conforming to the USGA Symmetry Rule are judged to be non-conforming to the USGA Rules of Golf and are thus not allowed to be used in USGA sanctioned golf competitions.

[0017] These golf balls with asymmetric dimples patterns or with manipulated weight distributions may be effective in reducing dispersion caused by a slice shot, but they also have their limitations, most notably the fact that they do not conform with the USGA Rules of Golf and that these balls must be oriented a certain way prior to club impact in order to display their maximum effectiveness.

[0018] The method of using a hard cover material or hard boundary layer material or slippery cover will reduce to a small extent the dispersion caused by a slice shot, but often does so at the expense of other desirable properties such as the ball spin rate off of short irons or the higher cost required to produce a multi-piece ball.

SUMMARY

[0019] A low lift golf ball is described herein.

[0020] According to one aspect, a golf ball having a plurality of dimples formed on its outer surface, the outer surface of the golf ball being divided into first and second areas each containing a plurality of dimples, the first and second areas being of different shapes, each first area containing first dimples and each second area containing second dimples, at least some first dimples being of different types from the second dimples, and the first areas being formed of circular paths around the outer surface of the ball, the second areas being formed by the intersection of the circular paths.

[0021] These and other features, aspects, and embodiments are described below in the section entitled "Detailed Description."

BRIEF DESCRIPTION OF THE DRAWINGS

[0022] Features, aspects, and embodiments are described in conjunction with the attached drawings, in which:

[0023] Figure 1 is a graph of the total spin rate versus the ball spin axis for various commercial and prototype golf balls hit with a driver at club head speed between 85-105 mph;

[0024] Figure 2 is a picture of golf ball with a dimple pattern in accordance with one embodiment;

[0025] Figure 3 is a top-view schematic diagram of a golf ball with a cuboctahedron pattern in accordance with one embodiment and in the poles-forward-backward (PFB) orientation;

[0026] Figure 4 is a schematic diagram showing the triangular polar region of another embodiment of the golf ball with a cuboctahedron pattern of figure 3;

[0027] Figure 5 is a graph of the total spin rate and Reynolds number for the TopFlite XL Straight golf ball and a B2 prototype ball, configured in accordance with one embodiment, hit with a driver club using a Golf Labs robot;

[0028] Figure 6 is a graph or the Lift Coefficient versus Reynolds Number for the golf ball shots shown in figure 5;

[0029] Figure 7 is a graph of Lift Coefficient versus flight time for the golf ball shots shown in figure 5;

[0030] Figure 8 is a graph of the Drag Coefficient versus Reynolds Number for the golf ball shots shown in figure 5;

[0031] Figures 9 is a graph of the Drag Coefficient versus flight time for the golf ball shots shown in figure 5;

[0032] Figure 10 is a diagram illustrating the relationship between the chord depth of a truncated and a spherical dimple in accordance with one embodiment;

[0033] Figure 11 is a graph illustrating the max height versus total spin for all of a 172-175 series golf balls, configured in accordance with certain embodiments, and the Pro V1 ® when hit with a driver imparting a slice on the golf balls;

[0034] Figure 12 is a graph illustrating the carry dispersion for the balls tested and shown in figure 11;

[0035] Figure 13 is a graph of the carry dispersion versus initial total spin rate for a golf ball with the 172 dimple pattern and the ProV1® for the same robot test data shown in figure 11;

[0036] Figure 14 is a graph of the carry dispersion versus initial total spin rate for a golf ball with the 173 dimple pattern and the ProV1® for the same robot test data shown in figure 11;

[0037] Figure 15 is a graph of the carry dispersion versus initial total spin rate for a golf ball with the 174 dimple pattern and the ProV1® for the same robot test data shown in figure 11;

[0038] Figure 16 is a graph of the carry dispersion versus initial total spin rate for a golf ball with the 175 dimple pattern and the ProV1® for the same robot test data shown in figure 11;

[0039] Figure 17 is a graph of the wind tunnel testing results showing Lift Coefficient (CL) versus DSP for the 173 golf ball against different Reynolds Numbers;

[0040] Figure 18 is a graph of the wind tunnel test results showing the CL versus DSP for the Pro V1 golf ball against different Reynolds Numbers;

[0041] Figure 19 is picture of a golf ball with a dimple pattern in accordance with another embodiment;

[0042] Figure 20 is a graph of the lift coefficient versus Reynolds Number at 3,000 rpm spin rate for the TopFlite® XL Straight, Pro V1®, 173 dimple pattern and a 273 dimple pattern in accordance with certain embodiments;

[0043] Figure 21 is a graph of the lift coefficient versus Reynolds Number at 3,500 rpm spin rate for the TopFlite® XL Straight, Pro V1®, 173 dimple pattern and 273 dimple pattern;

[0044] Figure 22 is a graph of the lift coefficient versus Reynolds Number at 4,000 rpm spin rate for the TopFlite® XL Straight, Pro V1®, 173 dimple pattern and 273 dimple pattern;

[0045] Figure 23 is a graph of the lift coefficient versus Reynolds Number at 4,500 rpm spin rate for the TopFlite® XL Straight, Pro V1®, 173 dimple pattern and 273 dimple pattern;

[0046] Figure 24 is a graph of the lift coefficient versus Reynolds Number at 5,000 rpm spin rate for the TopFlite® XL Straight, Pro V1®, 173 dimple pattern and 273 dimple pattern;

[0047] Figure 25 is a graph of the lift coefficient versus Reynolds Number at 4000 RPM initial spin rate for the 273 dimple pattern and 2-3 dimple pattern balls of Tables 10 and 11;

[0048] Figure 26 is a graph of the lift coefficient versus Reynolds Number at 4500 RPM initial spin rate for the 273 dimple pattern and 2-3 dimple pattern balls of Tables 10 and 11;

[0049] Figure 27 is a graph of the drag coefficient versus Reynolds Number at 4000 RPM initial spin rate for the 273 dimple pattern and 2-3 dimple pattern balls of Tables 10 and 11; and

[0050] Figure 28 is a graph of the drag coefficient versus Reynolds Number at 4500 RPM initial spin rate for the 273 dimple pattern and 2-3 dimple pattern balls of Tables 10 and 11.

DETAILED DESCRIPTION

[0051] The embodiments described herein may be understood more readily by reference to the following detailed description. However, the techniques, systems, and operating structures described can be embodied in a wide variety of forms and modes, some of which may be quite different from those in the disclosed embodiments. Consequently, the specific structural and functional details disclosed herein are merely representative. It must be noted that, as used in the specification and the appended claims, the singular forms "a", "an", and "the" include plural referents unless the context clearly indicates otherwise.

[0052] The embodiments described below are directed to the design of a golf ball that achieves low lift right after impact when the velocity and spin are relatively high. In particular, the embodiments described below achieve relatively low lift even when the spin rate is high, such as that imparted when a golfer slices the golf ball, e.g., 3500 rpm or higher. In the embodiments described below, the lift coefficient after impact can be as low as about .18 or less, and even less than .15 under such circumstances. In addition, the lift can be significantly lower than conventional golf balls at the end of flight, i.e., when the speed and spin are lower. For example, the lift coefficient can be less than .20 when the ball is nearing the end of flight.

[0053] As noted above, conventional golf balls have been designed for low initial drag and high lift toward the end of flight in order to increase distance. For example, U.S. Patent 6,224,499 to Ogg teaches and claims a lift coefficient greater than

.18 at a Reynolds number (Re) of 70,000 and a spin of 2000 rpm, and a drag coefficient less than .232 at a Re of 180,000 and a spin of 3000 rpm. One of skill in the art will understand that and Re of 70,000 and spin of 2000 rpm are industry standard parameters for describing the end of flight. Similarly, one of skill in the art will understand that a Re of greater than about 160,000, e.g., about 180,000, and a spin of 3000 rpm are industry standard parameters for describing the beginning of flight for a straight shot with only back spin.

[0054] The lift (CL) and drag coefficients (CD) vary by golf ball design and are generally a function of the velocity and spin rate of the golf ball. For a spherically symmetrical golf ball the lift and drag coefficients are for the most part independent of the golf ball orientation. The maximum height a golf ball achieves during flight is directly related to the lift force generated by the spinning golf ball while the direction that the golf ball takes, specifically how straight a golf ball flies, is related to several factors, some of which include spin rate and spin axis orientation of the golf ball in relation to the golf ball's direction of flight. Further, the spin rate and spin axis are important in specifying the direction and magnitude of the lift force vector.

[0055] The lift force vector is a major factor in controlling the golf ball flight path in the x, y, and z directions. Additionally, the total lift force a golf ball generates during flight depends on several factors, including spin rate, velocity of the ball relative to the surrounding air and the surface characteristics of the golf ball.

[0056] For a straight shot, the spin axis is orthogonal to the direction the ball is traveling and the ball rotates with perfect backspin. In this situation, the spin axis is 0 degrees. But if the ball is not struck perfectly, then the spin axis will be either positive (hook) or negative (slice). Figure 1 is a graph illustrating the total spin rate versus the spin axis for various commercial and prototype golf balls hit with a driver at club head speed between 85-105 mph. As can be seen, when the spin axis is negative, indicating a slice, the spin rate of the ball increases. Similarly, when the spin axis is positive, the spin rate decreases initially but then remains essentially constant with increasing spin axis.

[0057] The increased spin imparted when the ball is sliced, increases the lift coefficient (CL). This increases the lift force in a direction that is orthogonal to the spin axis. In other words, when the ball is sliced, the resulting increased spin produces an increased lift force that acts to "pull" the ball to the right. The more negative the spin axis, the greater the portion of the lift force acting to the right, and the greater the slice.

[0058] Thus, in order to reduce this slice effect, the ball must be designed to generate a relatively lower lift force at the greater spin rates generated when the ball is sliced.

[0059] Referring to Figure 2, there is shown golf ball 100, which provides a visual description of one embodiment of a dimple pattern that achieves such low initial lift at high spin rates. Figure 2 is a computer generated picture of dimple pattern 173. As shown in figure 2, golf ball 100 has an outer surface 105, which has a plurality of dissimilar dimple types arranged in a cuboctahedron configuration. In the example of figure 2, golf ball 100 has larger truncated dimples within square region 110 and smaller spherical dimples within triangular region 115 on the outer surface 105. The example of figure 2 and other embodiments are described in more detail below; however, as will be explained, in operation, dimple patterns configured in accordance with the embodiments described herein disturb the airflow in such a way as to provide a golf ball that exhibits low lift at the spin rates commonly seen with a slice shot as described above.

[0060] As can be seen, regions 110 and 115 stand out on the surface of ball 100 unlike conventional golf balls. This is because the dimples in each region are configured such that they have high visual contrast. This is achieved for example by including visually contrasting dimples in each area. For example, in one embodiment, flat, truncated dimples are included in region 110 while deeper, round or spherical dimples are included in region 115. Additionally, the radius of the dimples can also be different adding to the contrast.

[0061] But this contrast in dimples does not just produce a visually contrasting appearance; it also contributes to each region having a different aerodynamic effect. Thereby, disturbing air flow in such a manner as to produce low lift as described herein.

[0062] While conventional golf balls are often designed to achieve maximum distance by having low drag at high speed and high lift at low speed, when conventional golf balls are tested, including those claimed to be "straighter," it can be seen that these balls had quite significant increases in lift coefficients (CL) at the spin rates normally associated with slice shots. Whereas balls configured in accordance with the embodiments described herein exhibit lower lift coefficients at the higher spin rates and thus do not slice as much.

[0063] A ball configured in accordance with the embodiments described herein and referred to as the B2 Prototype, which is a 2-piece Surlyn-covered golf ball with a polybutadiene rubber based core and dimple pattern "273", and the TopFlite® XL Straight ball were hit with a Golf Labs robot using the same setup conditions so that the initial spin rates were about 3,400 - 3,500 rpm at a Reynolds Number of about 170,000. The spin rate and Re conditions near the end of the trajectory were about 2,900 to 3,200 rpm at a Reynolds Number of about 80,000. The spin rates and ball trajectories were obtained using a 3-radar unit Trackman Net System. Figure 5 illustrates the full trajectory spin rate versus Reynolds Number for the shots and balls described above.

[0064] The B2 prototype ball had dimple pattern design 273, shown in Figure 4. Dimple pattern design 273 is based on a cuboctahedron layout and has a total of 504 dimples. This is the inverse of pattern 173 since it has larger truncated dimples within triangular regions 115 and smaller spherical dimples within square regions or areas 110 on the outer surface of the ball. A spherical truncated dimple is a dimple which has a spherical side wall and a flat inner end, as seen in the triangular regions of Figure 4. The dimple patterns 173 and 273, and alternatives, are described in more detail below with reference to Tables 5 to 11.

[0065] Figure 6 illustrates the CL versus Re for the same shots shown in Figure 5; TopFlite® XL Straight and the B2 prototype golf ball which was configured in accordance with the systems and methods described herein. As can be seen, the B2 ball has a lower CL over the range of Re from about 75,000 to 170,000. Specifically, the CL for the B2 prototype never exceeds .27, whereas the CL for the TopFlite® XL Straight gets well above .27. Further, at a Re of about 165,000, the CL for the B2 prototype is about .16, whereas it is about .19 or above for the TopFlite® XL Straight.

[0066] Figures 5 and 6 together illustrate that the B2 ball with dimple pattern 273 exhibits significantly less lift force at spin rates that are associated with slices. As a result, the B2 prototype will be much straighter, i.e., will exhibit a much lower carry dispersion. For example, a ball configured in accordance with the embodiments described herein can have a CL of less than about .22 at a spin rate of 3,200-3,500 rpm and over a range of Re from about 120,000 to 180,000. For example, in certain embodiments, the CL can be less than .18 at 3500 rpm for Re values above about 155,000.

[0067] This is illustrated in the graphs of figures 20-24, which show the lift coefficient versus Reynolds Number at spin rates of 3,000 rpm, 3,500 rpm, 4,000 rpm, 4,500 rpm and 5,000 rpm, respectively, for the TopFlite® XL Straight, Pro V1®, 173 dimple pattern, and 273 dimple pattern. To obtain the regression data shown in figures 23-28, a Trackman Net System consisting of 3 radar units was used to track the trajectory of a golf ball that was struck by a Golf Labs robot equipped with various golf clubs. The robot was setup to hit a straight shot with various combinations of initial spin and velocity. A wind gauge was used to measure the wind speed at approximately 20 ft elevation near the robot location. The Trackman Net System measured trajectory data (x, y, z location vs. time) were then used to calculate the lift coefficients (CL) and drag coefficients (CD) as a function of measured time-dependent quantities including Reynolds Number, Ball Spin Rate, and Dimensionless Spin Parameter. Each golf ball model or design was tested under a range of velocity and spin conditions that included 3,000-5,000 rpm spin rate and 120,000-180,000 Reynolds Number. It will be understood that the Reynolds Number range of 150,000–180,000 covers the initial ball velocities typical for most recreational golfers, who have club head speeds of 85-100 mph. A 5-term multivariable regression model was then created from the data for each ball designed in accordance with the embodiments described herein for the lift and drag coefficients as a function of Reynolds Number (Re) and Dimensionless Spin Parameter (W), i.e., as a function of Re, W, Re^2, W^2, ReW, etc. Typically the predicted CD and CL values within the measured Re and W space (interpolation) were in close agreement with the measured CD and CL values. Correlation coefficients of >96% were typical.

[0068] Under typical slice conditions, with spin rates of 3,500 rpm or greater, the 173 and 273 dimple patterns exhibit lower lift coefficients than the other golf balls. Lower lift coefficients translate into lower trajectory for straight shots and less dispersion for slice shots. Balls with dimple patterns 173 and 273 have approximately 10% lower lift coefficients than the other golf balls under Re and spin conditions characteristics of slice shots. Robot tests show the lower lift coefficients result in at least 10% less dispersion for slice shots.

[0069] For example, referring again to figure 6, it can be seen that while the TopFlite® XL Straight is suppose to be a straighter ball, the data in the graph of figure 6 illustrates that the B2 prototype ball should in fact be much straighter based on its lower lift coefficient. The high CL for the TopFlite® XL Straight means that the TopFlite® XL Straight ball will create a larger lift force. When the spin axis is negative, this larger lift force will cause the TopFlite® XL Straight to go farther right increasing the dispersion for the TopFlite® XL Straight. This is illustrated in Table 2:

Ball	Dispersion, ft	Distance, yds
TopFlite® XL Straight	95.4	217.4
Ball 173	78.1	204.4

TABLE 2

[0070] Figure 7 shows that for the robot test shots shown in figure 5 the B2 ball has a lower CL throughout the flight time as compared to other conventional golf balls, such as the TopFlite® XL Straight. This lower CL throughout the flight of the ball translates in to a lower lift force exerted throughout the flight of the ball and thus a lower dispersion for a slice shot.

[0071] As noted above, conventional golf ball design attempts to increase distance, by decreasing drag immediately after impact. Figure 8 shows the drag coefficient (CD) versus Re for the B2 and TopFlite® XL Straight shots shown in figure 5. As can be seen, the CD for the B2 ball is about the same as that for the TopFlite® XL Straight at higher Re. Again, these higher Re numbers would occur near impact. At lower Re, the CD for the B2 ball is significantly less than that of the TopFlite® XL Straight.

[0072] In figure 9 it can be seen that the CD curve for the B2 ball throughout the flight time actually has a negative inflection in the middle. Thus, the drag for the B2 ball will be less in the middle of the ball's flight as compared to the TopFlite XL Straight. It should also be noted that while the B2 does not carry quite as far as the TopFlite XL Straight, testing reveals that it actually roles farther and therefore the overall distance is comparable under many conditions. This makes sense of course because the lower CL for the B2 ball means that the B2 ball generates less lift and therefore does not fly as high, something that is also verified in testing. Because the B2 ball does not fly as high, it impacts the ground at a shallower angle, which results in increased role.

[0073] Returning to figures 2-4, the outer surface 105 of golf ball 100 can include dimple patterns of Archimedean solids or Platonic solids by subdividing the outer surface 105 into patterns based on a truncated tetrahedron, truncated cube, truncated octahedron, truncated dodecahedron, truncated icosahedron, icosidodecahedron, rhombicuboctahedron, rhombicosidodecahedron, rhombitruncated cuboctahedron, rhombitruncated icosidodecahedron, snub cube, snub dodecahedron, cube, dodecahedron, icosahedrons, octahedron, tetrahedron, where each has at least two types of subdivided regions (A and B) and each type of region has its own dimple pattern and types of dimples that are different than those in the other type region or regions.

[0074] Furthermore, the different regions and dimple patterns within each region are arranged such that the golf ball 100 is spherically symmetrical as defined by the United States Golf Association ("USGA") Symmetry Rules. It should be appreciated that golf ball 100 may be formed in any conventional manner such as, in one non-limiting example, to include two pieces having an inner core and an outer cover. In other non-limiting examples, the golf ball 100 may be formed of three, four or more pieces.

[0075] Tables 3 and 4 below list some examples of possible spherical polyhedron shapes which may be used for golf ball 100, including the cuboctahedron shape illustrated in figures 2-4. The size and arrangement of dimples in different regions in the other examples in Tables 3 and 4 can be similar or identical to that of figure 2 or 4.

13 Archimedean Solids and 5 Platonic solids - relative surface areas for the polygonal patches

Name of Archimedean solid	# of Region A	Region A shape	% surface area for all of the Region A's	# of Region B	Region B shape	% surface area for all of the Region B's	# of Region C	Region C shape	% surface area for all of the Region C's	Total number of Regions	% surface area per single A Region	% surface area per single B Region	% surface area per single C Region
truncated icosidodeca-hedron	30	triangles	17%	20	Hexagons	30%	12	decagons	53%	62	0.6%	1.5%	4.4%
Rhombicosidodeca-hedron	20	triangles	15%	30	squares	51%	12	pentagons	35%	62	0.7%	1.7%	2.9%
snub dodeca-hedron	80	triangles	63%	12	Pentagons	37%				92	0.8%	3.1%	
truncated icosahedron	12	pentagons	28%	20	Hexagons	72%				32	2.4%	3.6%	
truncated cubocta-hedron	12	squares	19%	8	Hexagons	34%	6	octagons	47%	26	1.6%	4.2%	7.8%
Rhombicub-octahedron	8	triangles	16%	18	squares	84%				26	2.0%	4.7%	
snub cube	32	triangles	70%	6	squares	30%				38	2.2%	5.0%	
Icosado-decahedron	20	triangles	30%	12	Pentagons	70%				32	1.5%	5.9%	
truncated dodeca-hedron	20	triangles	9%	12	Decagons	91%				32	0.4%	7.6%	
truncated octahedron	6	squares	22%	8	Hexagons	78%				14	3.7%	9.7%	
Cubocta-hedron	8	triangles	37%	6	squares	63%				14	4.6%	10.6%	
truncated cube	8	triangles	11%	6	Octagons	89%				14	1.3%	14.9%	
truncated tetrahedron	4	triangles	14%	4	Hexagons	86%				8	3.6%	21.4%	

TABLE 3

Name of Platonic Solid	# of Regions	Shape of Regions		Surface area per Region
Tetrahedral Sphere	4	triangle	100%	25%
Octahedral Sphere	8	triangle	100%	13%
Hexahedral Sphere	6	squares	100%	17%
Icosahedral Sphere	20	triangles	100%	5%
Dodecahadral Sphere	12	pentagons	100%	8%

TABLE 4

[0076] Figure 3 is a top-view schematic diagram of a golf ball with a cuboctahedron pattern illustrating a golf ball, which may be ball 100 of Figure 2 or ball 273 of Figure 4, in the poles-forward-backward (PFB) orientation with the equator 130 (also called seam), oriented in a vertical plane 220 that points to the right/left and up/down, with pole 205 pointing straight forward and orthogonal to equator 130, and pole 210 pointing straight backward, i.e., approximately located at the point of club impact. In this view, the tee upon which the golf ball 100 would be resting would be located in the center of the golf ball 100 directly below the golf ball 100 (which is out of view in this figure). In addition, outer surface 105 of golf ball 100 has two types of regions of dissimilar dimple types arranged in a cuboctahedron configuration. In the cuboctahedral dimple pattern 173, outer surface 105 has larger dimples arranged in a plurality of three square regions 110 while smaller dimples are arranged in the plurality of four triangular regions 115 in the front hemisphere 120 and back hemisphere 125 respectively for a total of six square regions and eight triangular regions arranged on the outer surface 105 of the golf ball 100. In the inverse cuboctahedral dimple pattern 273, outer surface 105 has larger dimples arranged in the eight triangular regions and smaller dimples arranged in the total of six square regions. In either case, the golf ball 100 contains 504 dimples. In golf ball 173, each of the triangular regions and the square regions containing thirty-six dimples. In golf ball 273, each triangular region contains fifteen dimples while each square region contains sixty four dimples. Further, the top hemisphere 120 and the bottom hemisphere 125 of golf ball 100 are identical and are rotated 60 degrees from each other so that on the equator 130 (also called seam) of the golf ball 100, each square region 110 of the front hemisphere 120 borders each triangular region 115 of the back hemisphere 125. Also shown in Figure 4, the back pole 210 and front pole (not shown) pass through the triangular region 115 on the outer surface 105 of golf ball 100.

[0077] Accordingly, a golf ball 100 designed in accordance with the embodiments described herein will have at least two different regions A and B comprising different dimple patterns and types. Depending on the embodiment, each region A and B, and C where applicable, can have a single type of dimple, or multiple types of dimples. For example, region A can have large dimples, while region B has small dimples, or vice versa; region A can have spherical dimples, while region B has truncated dimples, or vice versa; region A can have various sized spherical dimples, while region B has various sized truncated dimples, or vice versa, or some combination or variation of the above. Some specific example embodiments are described in more detail below.

[0078] It will be understood that there is a wide variety of types and construction of dimples, including non-circular dimples, such as those described in U.S. Patent 6,409,615, hexagonal dimples, dimples formed of a tubular lattice structure, such as those described in U.S. Patent 6,290,615, as well as more conventional dimple types. It will also be understood that any of these types of dimples can be used in conjunction with the embodiments described herein. As such, the term "dimple" as used in this description and the claims that follow is intended to refer to and include any type of dimple or dimple construction, unless otherwise specifically indicated.

[0079] It should also be understood that a golf ball designed in accordance with the embodiments described herein can be configured such that the average volume per dimple in one region, e.g., region A, is greater than the average volume per dimple in another regions, e.g., region B. Also, the unit volume in one region, e.g., region A, can be greater, e.g., 5% greater, 15% greater, etc., than the average unit volume in another region, e.g., region B. The unit volume can be defined as the volume of the dimple sin one region divided by the surface area of the region. Also, the regions do not have to be perfect geometric shapes. For example, the triangle areas can incorporate, and therefore extend into, a small number of dimple form the adjacent square region, or vice versa. Thus, an edge of the triangle region can extend out in a tab like fashion into the adjacent square region. This could happen on one or more than one edge of one or more than one region. In this way, the areas can be said to be derived based on certain geometric shapes, i.e., the underlying shape is still a triangle or square, but with some irregularities at the edges. Accordingly, in the specification and claims that follow when a region is said to be, e.g., a triangle region, this should also be understood to cover a region that is of a shape derived from a triangle.

[0080] But first, Figure 10 is a diagram illustrating the relationship between the chord depth of a truncated and a spherical dimple. The golf ball having a preferred diameter of about 1.68 inches contains 504 dimples to form the cuboctahedral pattern, which was shown in figures 2-4. As an example of just one type of dimple, figure 12 shows truncated dimple 400 compared to a spherical dimple having a generally spherical chord depth of 0.012 inches and a radius of 0.075 inches. The truncated dimple 400 may be formed by cutting a spherical indent with a flat inner end, i.e. corresponding to spherical dimple 400 cut along plane A—A to make the dimple 400 more shallow with a flat inner end, and having a truncated chord depth smaller than the corresponding spherical chord depth of 0.012 inches.

[0081] The dimples can be aligned along geodesic lines with six dimples on each edge of the square regions, such as square region 110, and eight dimples on each edge of the triangular region 115. The dimples can be arranged according to the three-dimensional Cartesian coordinate system with the X-Y plane being the equator of the ball and the Z direction passing through the pole of the golf ball 100. The angle Φ is the circumferential angle while the angle θ is the co-latitude with 0 degrees at the pole and 90 degrees at the equator. The dimples in the North hemisphere can be offset by 60 degrees from the South hemisphere with the dimple pattern repeating every 120 degrees. Golf ball 100, in the example of figure 2, has a total of nine dimple types, with four of the dimple types in each of the triangular regions and five of the dimple types in each of the square regions. As shown in Table 5 below, the various dimple depths and profiles are given for various implementations of golf ball 100, indicated as prototype codes 173-175. The actual location of each dimple on the surface of the ball for dimple patterns 172-175 is given in Tables 6-9. Tables 10 and 11 provide the various dimple depths and profiles for dimple pattern 273 of Figure 4 and an alternative dimple pattern 2-3, respectively, as well as the location of each dimple on the ball for each of these dimple patterns. Dimple pattern 2-3 is similar to dimple pattern 273 but has dimples of slightly larger chord depth than the ball with dimple pattern 273, as shown in Table 11.

Ball 175									
Dimple ID#	1	2	3	4	5	6	7	8	9
Type Dimple Region	Triangle	Triangle	Triangle	Triangle	Square	Square	Square	Square	Square
Type Dimple	spherical	spherical	spherical	spherical	truncated	truncated	truncated	truncated	truncated
Dimple Radius, in	0.05	0.0525	0.055	0.0575	0.075	0.0775	0.0825	0.0875	0.095
Spherical Chord Depth, in	0.008	0.008	0.008	0.008	0.012	0.0122	0.0128	0.0133	0.014
Truncated Chord Depth, in	n/a	n/a	n/a	n/a	0.0035	0.0035	0.0035	0.0035	0.0035
# of dimples in region	9	18	6	3	12	8	8	4	4

Ball 174									
Dimple ID#	1	2	3	4	5	6	7	8	9
Type Dimple Region	Triangle	Triangle	Triangle	Triangle	Square	Square	Square	Square	Square
Type Dimple	truncated	truncated	truncated	truncated	spherical	spherical	spherical	spherical	spherical
Dimple Radius, in	0.05	0.0525	0.055	0.0575	0.075	0.0775	0.0825	0.0875	0.095
Spherical Chord Depth, in	0.0087	0.0091	0.0094	0.0098	0.008	0.008	0.008	0.008	0.008
Truncated Chord Depth, in	0.0035	0.0035	0.0035	0.0035	n/a	n/a	n/a	n/a	n/a
# of dimples in region	9	18	6	3	12	8	8	4	4

Ball 173									
Dimple ID#	1	2	3	4	5	6	7	8	9
Type Dimple Region	Triangle	Triangle	Triangle	Triangle	Square	Square	Square	Square	Square
Type Dimple	spherical	spherical	spherical	spherical	truncated	truncated	truncated	truncated	truncated
Dimple Radius, in	0.05	0.0525	0.055	0.0575	0.075	0.0775	0.0825	0.0875	0.095
Spherical Chord Depth, in	0.0075	0.0075	0.0075	0.0075	0.012	0.0122	0.0128	0.0133	0.014
Truncated Chord Depth, in	n/a	n/a	n/a	n/a	0.005	0.005	0.005	0.005	0.005
# of dimples in region	9	18	6	3	12	8	8	4	4

Ball 172									
Dimple ID#	1	2	3	4	5	6	7	8	9
Type Dimple Region	Triangle	Triangle	Triangle	Triangle	Square	Square	Square	Square	Square
Type Dimple	spherical	spherical	spherical	spherical	spherical	spherical	spherical	spherical	spherical
Dimple Radius, in	0.05	0.0525	0.055	0.0575	0.075	0.0775	0.0825	0.0875	0.095
Spherical Chord Depth, in	0.0075	0.0075	0.0075	0.0075	0.005	0.005	0.005	0.005	0.005
Truncated Chord Depth, in	n/a	n/a	n/a	n/a	n/a	n/a	n/a	n/a	n/a
# of dimples in region	9	18	6	3	12	8	8	4	4

TABLE 5

Dimple #	1	
Type	spherical	
Radius	0.05	
SCD	0.0075	
TCD	n/a	
#	**Phi**	**Theta**
1	0	28.81007
2	0	41.7187
3	5.308533	47.46948
4	9.848338	23.49139
5	17.85912	86.27884
6	22.3436	79.84939
7	24.72264	86.27886
8	95.27736	86.27886
9	97.6564	79.84939
10	102.1409	86.27884
11	110.1517	23.49139
12	114.6915	47.46948
13	120	28.81007
14	120	41.7187
15	125.3085	47.46948
16	129.8483	23.49139
17	137.8591	86.27884
18	142.3436	79.84939
19	144.7226	86.27886
20	215.2774	86.27886
21	217.6564	79.84939
22	222.1409	86.27884
23	230.1517	23.49139
24	234.6915	47.46948
25	240	28.81007
26	240	41.7187
27	245.3085	47.46948
28	249.8483	23.49139
29	257.8591	86.27884
30	262.3436	79.84939
31	264.7226	86.27886
32	335.2774	86.27886
33	337.6564	79.84939
34	342.1409	86.27884
35	350.1517	23.49139
36	354.6915	47.46948

Dimple #	2	
Type	spherical	
Radius	0.0525	
SCD	0.0075	
TCD	n/a	
#	**Phi**	**Theta**
1	3.606874	86.10963
2	4.773603	59.66486
3	7.485123	79.72027
4	9.566953	53.68971
5	10.81146	86.10963
6	12.08533	72.79786
7	13.37932	60.13101
8	16.66723	66.70139
9	19.58024	73.34845
10	20.76038	11.6909
11	24.53367	18.8166
12	46.81607	15.97349
13	73.18393	15.97349
14	95.46633	18.8166
15	99.23962	11.6909
16	100.4198	73.34845
17	103.3328	66.70139
18	106.6207	60.13101
19	107.9147	72.79786
20	109.1885	86.10963
21	110.433	53.68971
22	112.5149	79.72027
23	115.2264	59.66486
24	116.3931	86.10963
25	123.6069	86.10963
26	124.7736	59.66486
27	127.4851	79.72027
28	129.567	53.68971
29	130.8115	86.10963
30	132.0853	72.79786
31	133.3793	60.13101
32	136.6672	66.70139
33	139.5802	73.34845
34	140.7604	11.6909
35	144.5337	18.8166
36	166.8161	15.97349
37	193.1839	15.97349
38	215.4663	18.8166
39	219.2396	11.6909
40	220.4198	73.34845
41	223.3328	66.70139
42	226.6207	60.13101
43	227.9147	72.79786
44	229.1885	86.10963
45	230.433	53.68971
46	232.5149	79.72027
47	235.2264	59.66486
48	236.3931	86.10963
49	243.6069	86.10963
50	244.7736	59.66486
51	247.4851	79.72027
52	249.567	53.68971
53	250.8115	86.10963
54	252.0853	72.79786
55	253.3793	60.13101
56	256.6672	66.70139
57	259.5802	73.34845

Dimple #	3	
Type	spherical	
Radius	0.055	
SCD	0.0075	
TCD	n/a	
#	**Phi**	**Theta**
1	0	17.13539
2	0	79.62325
3	0	53.39339
4	8.604739	66.19316
5	15.03312	79.65081
6	60	9.094473
7	104.9669	79.65081
8	111.3953	66.19316
9	120	17.13539
10	120	53.39339
11	120	79.62325
12	128.6047	66.19316
13	135.0331	79.65081
14	180	9.094473
15	224.9669	79.65081
16	231.3953	66.19316
17	240	17.13539
18	240	53.39339
19	240	79.62325
20	248.6047	66.19316
21	255.0331	79.65081
22	300	9.094473
23	344.9669	79.65081
24	351.3953	66.19316

TABLE 6 (Dimple Pattern 172)

Dimple #	2 (cont'd)	
#	**Phi**	**Theta**
58	260.7604	11.6909
59	264.5337	18.8166
60	286.8161	15.97349
61	313.1839	15.97349
62	335.4663	18.8166
63	339.2396	11.6909
64	340.4198	73.34845
65	343.3328	66.70139
66	346.6207	60.13101
67	347.9147	72.79786
68	349.1885	86.10963
69	350.433	53.68971
70	352.5149	79.72027
71	355.2264	59.66486
72	356.3931	86.10963

TABLE 6 (Dimple Pattern 172) (continued)

Dimple #	4	
Type	spherical	
Radius	0.075	
SCD	0.005	
TCD	n/a	
#	**Phi**	**Theta**
1	0	4.637001
2	0	65.89178
3	4.200798	72.89446
4	115.7992	72.89446
5	120	4.637001
6	120	65.89178
7	124.2008	72.89446
8	235.7992	72.89446
9	240	4.637001
10	240	65.89178
11	244.2008	72.89446
12	355.7992	72.89446

Dimple #	5	
Type	spherical	
Radius	0.075	
SCD	0.005	
TCD	n/a	
#	**Phi**	**Theta**
1	11.39176	35.80355
2	17.86771	45.18952
3	26.35389	29.36327
4	30.46014	74.86406
5	33.84232	84.58637
6	44.16317	84.58634
7	75.83683	84.58634
8	86.15768	84.58637
9	89.53986	74.86406
10	93.64611	29.36327
11	102.1323	45.18952
12	108.6082	35.80355
13	131.3918	35.80355
14	137.8677	45.18952
15	146.3539	29.36327
16	150.4601	74.86406
17	153.8423	84.58637
18	164.1632	84.58634
19	195.8368	84.58634
20	206.1577	84.85637
21	209.5399	74.86406
22	213.6461	29.36327
23	222.1323	45.18952
24	228.6082	35.80355
25	251.3918	35.80355
26	257.8677	45.18952
27	266.3539	29.36327
28	270.4601	74.86406
29	273.8423	84.58637
30	284.1632	84.58634
31	315.8368	84.58634
32	326.1577	84.58637
33	329.5399	74.86406
34	333.6461	29.36327
35	342.1323	45.18952
36	348.6082	35.80355

Dimple #	6	
Type	spherical	
Radius	0.0775	
SCD	0.005	
TCD	n/a	
#	**Phi**	**Theta**
1	22.97427	54.90551
2	27.03771	64.89835
3	47.66575	25.59568
4	54.6796	84.41703
5	65.3204	84.41703
6	72.33425	25.59568
7	92.96229	64.89835
8	97.02573	54.90551
9	142.9743	54.90551
10	147.0377	64.89835
11	167.6657	25.59568
12	174.6796	84.41703
13	185.3204	84.41703
14	192.3343	25.59568
15	212.9623	64.89835
16	217.0257	54.90551
17	262.9743	54.90551
18	267.0377	64.89835
19	287.6657	25.59568
20	294.6796	84.41703
21	305.3204	84.41703
22	312.3343	25.59568
23	332.9623	64.89835
24	337.0257	54.90551

TABLE 6 (Dimple Pattern 172) (continued)

Dimple #	7	
Type	spherical	
Radius	0.0825	
SCD	0.005	
TCD	n/a	
#	**Phi**	**Theta**
1	35.91413	51.35559
2	38.90934	62.34835
3	50.48062	36.43373
4	54.12044	73.49879
5	65.87956	73.49879
6	69.51938	36.43373
7	81.09066	62.34835
8	84.08587	51.35559
9	155.9141	51.35559
10	158.9093	62.34835
11	170.4806	36.43373
12	174.1204	73.49879
13	185.8796	73.49879
14	189.5194	36.43373
15	201.0907	62.34835
16	204.0859	51.35559
17	275.9141	51.35559
18	278.9093	62.34835
19	290.4806	36.43373
20	294.1204	73.49879
21	305.8796	73.49879
22	309.5194	36.43373
23	321.0907	62.34835
24	324.0859	51.35559

Dimple #	8	
Type	spherical	
Radius	0.0875	
SCD	0.005	
TCD	n/a	
#	**Phi**	**Theta**
1	32.46033	39.96433
2	41.97126	73.6516
3	78.02874	73.6516
4	87.53967	39.96433
5	152.4603	39.96433
6	161.9713	73.6516
7	198.0287	73.6516
8	207.5397	39.96433
9	272.4603	39.96433
10	281.9713	73.6516
11	318.0287	73.6516
12	327.5397	39.96433

Dimple #	9	
Type	spherical	
Radius	0.095	
SCD	0.005	
TCD	n/a	
#	**Phi**	**Theta**
1	51.33861	48.53996
2	52.61871	61.45814
3	67.38129	61.45814
4	68.66139	48.53996
5	171.3386	48.53996
6	172.6187	61.45814
7	187.3813	61.45814
8	188.6614	48.53996
9	291.3386	48.53996
10	292.6187	61.45814
11	307.3813	61.45814
12	308.6614	48.53996

TABLE 6 (Dimple Pattern 172) (continued)

Dimple #	1
Type	spherical
Radius	0.05
SCD	0.0075
TCD	n/a

#	Phi	Theta
1	0	28.81007
2	0	41.7187
3	5.30853345	47.46948
4	9.848337904	23.49139
5	17.85912075	86.27884
6	22.34360082	79.84939
7	24.72264341	86.27886
8	95.27735659	86.27886
9	97.65639918	79.849.39
10	102.1408793	86.27884
11	110.1516621	23.49139
12	114.6914665	47.46948
13	120	28.81007
14	120	41.7187
15	125.3085335	47.46948
16	129.8483379	23.49139
17	137.8591207	86.27884
18	142.3436008	79.84939
19	144.7226434	86.27886
20	215.2773566	86.27886
21	217.6563991	79.84939
22	222.1408793	86.27884
23	230.1516621	23.49139
24	234.6914665	47.46948
25	240	28.81007
26	240	41.7187
27	245.3085335	47.46948
28	249.8483379	23.49139
29	257.8591207	86.27884
30	262.3436008	79.84939
31	264.7226434	86.27886
32	335.2773566	86.27886
33	337.6563992	79.84939
34	342.1408793	86.27884
35	350.1516621	23.49139
36	354.6914665	47.46948

Dimple #	2
Type	spherical
Radius	0.0525
SCD	0.0075
TCD	n/a

#	Phi	Theta
1	3.606873831	86.10963
2	4.773603104	59.66486
3	7.485123389	79.72027
4	9.566952638	53.68971
5	10.81146128	86.10963
6	12.08533241	72.79786
7	13.37931975	60.13101
8	16.66723032	66.70139
9	19.58024114	73.34845
10	20.76038062	11.6909
11	24.53367306	18.8166
12	46.81607116	15.97349
13	73.18392884	15.97349
14	95.46632694	18.8166
15	99.23961938	11.6909
16	100.4197589	73.34845
17	103.3327697	66.70139
18	106.6206802	60.13101
19	107.9146676	72.79786
20	109.1885387	86.10963
21	110.4330474	53.68971
22	112.5148766	79.72027
23	115.2263969	59.66486
24	116.3931262	86.10963
25	123.6068738	86.10963
26	124.7736031	59.66486
27	127.4851234	79.72027
28	129.5669526	53.68971
29	130.8114613	86.10963
30	132.0853324	72.79786
31	133.3793198	60.13101
32	136.6672303	66.70139
33	139.5802411	73.34845
34	140.7603806	11.6909
35	144.5336731	18.8166
36	166.8160712	15.97349
37	193.1839288	15.97349
38	215.4663269	18.8166
39	219.2396194	11.6909
40	220.4197589	73.34845
41	223.3327697	66.70139
42	226.6206802	60.13101
43	227.9146676	72.79786
44	229.1885387	86.10963
45	230.4330474	53.68971
46	232.5148766	79.72027
47	235.2263969	59.66486
48	236.3931262	86.10963
49	243.6068738	86.10963
50	244.7736031	59.66486
51	247.4851234	79.72027
52	249.5669526	53.68971
53	250.6114613	86.10963
54	252.0853324	72.79786
55	253.3793198	60.13101
56	256.6672303	66.70139
57	259.5802411	73.34845

Dimple #	3
Type	spherical
Radius	0.055
SCD	0.0075
TCD	n/a

#	Phi	Theta
1	0	17.13539
2	0	79.62325
3	0	53.39339
4	8.604738835	66.19316
5	15.03312161	79.65081
6	60	9.094473
7	104.9668784	79.65081
8	111.3952612	66.19316
9	120	17.13539
10	120	53.39339
11	120	79.62325
12	128.6047388	66.19316
13	135.0331216	79.65081
14	180	9.094473
15	224.9668784	79.65081
16	231.3952612	66.19316
17	240	17.13539
18	240	53.39339
19	240	79.62325
20	248.6047388	66.19316
21	255.0331215	79.65081
22	300	9.094473
23	344.9668784	79.65081
24	351.3952612	66.19316

TABLE 7 (Dimple Pattern 173)

Dimple #	2 (cont'd)	
#	**Phi**	**Theta**
58	260.7603806	11.6909
59	264.5336731	18.8166
60	286.8160712	15.97349
61	313.1839288	15.97349
62	335.4663269	18.8166
63	339.2396194	11.6909
64	340.4197589	73.34845
65	343.3327697	66.70139
66	346.6206802	60.13101
67	347.9146676	72.79786
68	349.1885387	86.10963
69	350.4330474	53.68971
70	352.5148766	79.72027
71	355.2663969	59.66486
72	356.3931262	86.10953

TABLE 7 (Dimple Pattern 173) (continued)

Dimple #	4	
Type	spherical	
Radius	0.075	
SCD	0.005	
TCD	n/a	
#	**Phi**	**Theta**
1	0	4.637001
2	0	65.89178
3	4.200798314	72.89446
4	115.7992017	72.89446
5	120	4.637001
6	120	65.89178
7	124.2007983	72.89446
8	235.7992017	72.89446
9	240	4.637001
10	240	65.89178
11	244.2007983	72.89446
12	355.7992017	72.89446

Dimple #	5	
Type	truncated	
Radius	0.075	
SCD	0.0119	
TCD	0.005	
#	**Phi**	**Theta**
1	11.39176224	35.80355
2	17.86771474	45.18952
3	26.35389345	29.36327
4	30.46014274	74.86406
5	33.84232422	84.58637
6	44.16316958	84.58634
7	75.83683042	84.58634
8	86.15767578	84.58637
9	89.53985726	74.86406
10	93.64610655	29.36327
11	102.1322853	45.18952
12	108.6082378	35.80355
13	131.3917622	35.80355
14	137.8677147	45.18952
15	146.3538935	29.36327
16	150.4601427	74.86406
17	153.8423242	84.58637
18	164.1631696	84.58634
19	195.8368304	84.58634
20	206.1576750	84.58637
21	209.5398573	74.86406
22	213.6461065	29.36327
23	222.1322853	45.18952
24	228.6082378	35.80355
25	251.3917622	35.80355
26	257.8677147	45.18952
27	266.3538935	29.36327
28	270.4801427	74.86406
29	273.8423242	84.58637
30	284.1631696	84.58634
31	315.8368304	84.58634
32	326.1576758	84.58637
33	329.5398573	74.86406
34	333.6461065	29.36327
35	342.1322853	45.18952
36	348.6082378	35.80355

Dimple #	6	
Type	truncated	
Radius	0.0775	
SCD	0.0122	
TCD	0.005	
#	**Phi**	**Theta**
1	22.97426943	54.90551
2	27.03771469	64.89835
3	47.6657487	25.59568
4	54.67960187	84.41703
5	65.32039813	84.41703
6	72.3342513	25.59568
7	92.96228531	64.89835
8	97.02573057	54.90551
9	142.9742694	54.90551
10	147.0377147	64.89835
11	167.6657487	25.59568
12	174.6796019	84.41703
13	185.3203981	84.41703
14	192.3342513	25.59568
15	212.9622853	64.89835
16	217.0257306	54.90551
17	262.9742694	54.90551
18	267.0377147	64.89835
19	297.6657487	25.59568
20	294.6796019	84.41703
21	305.3203981	84.41703
22	312.3342513	25.59568
23	332.9622853	64.89835
24	337.0257306	54.90551

TABLE 7 (Dimple Pattern 173) (continued)

Dimple #	7		**Dimple #**	8		**Dimple #**	9	
Type	truncated		**Type**	truncated		**Type**	truncated	
Radius	0.0825		**Radius**	0.0875		**Radius**	0.095	
SCD	0.0128		**SCD**	0.0133		**SCD**	0.014	
TCD	0.005		**TCD**	0.005		**TCD**	0.005	
#	**Phi**	**Theta**	**#**	**Phi**	**Theta**	**#**	**Phi**	**Theta**
1	35.91413117	51.35559	1	32.46032855	39.96433	1	51.33861068	48.53996
2	38.90934195	62.34835	2	41.97126436	73.6516	2	52.61871427	61.45814
3	50.48062345	36.43373	3	78.02873564	73.6516	3	67.38128573	61.45814
4	54.12044072	73.49879	4	87.53967145	39.96433	4	68.66138932	48.53996
5	65.87955928	73.49879	5	152.4603285	39.96433	5	171.3386107	48.53996
6	69.51937655	36.43373	6	161.9712644	73.6516	6	172.6187143	61.45814
7	81.09065805	62.34835	7	198.0287356	73.6516	7	187.3812857	61.45814
8	84.08586883	51.35559	8	207.5396715	39.96433	8	188.6613893	48.53996
9	155.9141312	51.35559	9	272.4603285	39.96433	9	291.3386107	48.53996
10	158.909342	62.34835	10	281.9712644	73.6516	10	292.6187143	61.45814
11	170.4806234	36.43373	11	318.0287356	73.6516	11	307.3812857	61.45814
12	174.1204407	73.49879	12	327.5396715	39.96433	12	308.6613893	48.53996
13	185.8795593	73.49879						
14	189.5193766	36.43373						
15	201.090658	62.34835						
16	204.0858688	51.35559						
17	275.9141312	51.35559						
18	278.909342	62.34835						
19	290.4806234	36.43373						
20	294.1204407	73.49879						
21	305.8795593	73.49879						
22	309.5193766	36.43373						
23	321.090658	62.34835						
24	324.0858688	51.35559						

TABLE 7 (Dimple Pattern 173) (continued)

Dimple #	1	
Type	truncated	
Radius	0.05	
SCD	0.0087	
TCD	0.0035	
#	**Phi**	**Theta**
1	0	28.81007
2	0	41.7187
3	5.308533	47.46948
4	9.848338	23.49139
5	17.85912	86.27884
6	22.3436	79.84939
7	24.72264	86.27886
8	95.27736	86.27886
9	97.6564	79.84939
10	102.1409	86.27884
11	110.1517	23.49139
12	114.6915	47.46948
13	120	28.81007
14	120	41.7187
15	125.3085	47.46948
16	129.8483	23.49139
17	137.8591	86.27884
18	142.3436	79.84939
19	144.7226	86.27886
20	315.2774	86.27886
21	217.6564	79.84939
22	222.1409	86.27884
23	230.1517	23.49139
24	234.6915	47.46948
25	240	28.81007
26	240	41.7187
27	345.3085	47.46948
28	249.8483	23.49139
29	257.8591	86.27884
30	262.3436	79.84939
31	264.7226	86.27886
32	335.2774	86.27886
33	337.6564	79.84939
34	342.1409	86.27884
35	350.1517	23.49139
36	354.6915	47.46948

Dimple #	2	
Type	truncated	
Radius	0.0525	
SCD	0.0091	
TCD	0.0035	
#	**Phi**	**Theta**
1	3.606874	86.10963
2	4.773603	59.66486
3	7.485123	79.72027
4	9.566953	53.68971
5	10.81146	86.10963
6	12.08533	72.79786
7	13.37932	60.13101
8	16.66723	66.70139
9	19.58024	73.34545
10	20.76038	11.6909
11	24.53367	18.8166
12	46.81607	15.97349
13	73.18393	15.97349
14	95.46633	18.8166
15	99.23962	11.6909
16	100.4198	73.34845
17	103.3328	66.70139
18	106.6207	60.13101
19	107.9147	72.79786
20	109.1885	86.10963
21	110.433	53.68971
22	112.5149	79.72027
23	115.2264	59.66486
24	116.3931	86.10963
25	123.6069	86.10963
26	124.7736	59.66486
27	127.4851	79.72027
28	129.567	53.68971
29	130.8115	86.10963
30	132.0853	72.79786
31	133.3793	60.13101
32	136.6672	66.70139
33	139.5802	73.34845
34	140.7604	11.6909
35	144.5337	18.8166
36	166.8161	15.97349
37	193.1839	15.97349
38	215.4663	18.8166
39	219.2396	11.6909
40	220.4198	73.34845
41	223.3328	66.70139
42	226.6207	60.13101
43	227.9147	72.79786
44	229.1885	86.10963
45	230.433	53.68971
46	232.5149	79.72027
47	235.2264	59.66486
48	236.3931	86.10963
49	243.6069	86.10963
50	244.7736	59.66486
51	247.4851	79.72027
52	249.567	53.68971
53	250.8115	86.10963
54	252.0853	72.79786
55	253.3793	60.13101
56	256.6672	66.70139
57	259.5802	73.34845

Dimple #	3	
Type	truncated	
Radius	0.055	
SCD	0.0094	
TCD	0.0035	
#	**Phi**	**Theta**
1	0	17.13539
2	0	79.62325
3	0	53.39339
4	8.604739	66.19316
5	15.03312	79.65081
6	60	9.094473
7	104.9669	79.65081
8	111.3953	66.19316
9	120	17.13539
10	120	53.39339
11	120	79.62325
12	128.6047	66.19316
13	135.0331	79.65081
14	180	9.094473
15	224.9669	79.65081
16	231.3953	66.19316
17	240	17.13539
18	240	53.39339
19	240	79.62325
20	248.6047	66.19316
21	255.0331	79.65081
22	300	9.094473
23	344.9669	79.65081
24	351.3953	66.19316

TABLE 8 (Dimple Pattern 174)

Dimple #	2 (cont'd)	
#	**Phi**	**Theta**
58	260.7604	11.6909
59	264.5337	18.8166
60	286.8161	15.97349
61	313.1839	15.97349
62	335.4663	18.8166
63	339.2396	11.6909
64	340.4198	73.34845
65	343.3328	66.70139
66	346.6207	60.13101
67	347.9147	72.79786
68	349.1885	86.10963
69	350.433	53.68971
70	352.5149	79.72027
71	355.2264	59.66486
72	356.3931	86.10963

TABLE 8 (Dimple Pattern 174) (continued)

Dimple #	4	
Type	truncated	
Radius	0.0575	
SCD	0.0098	
TCD	0.0035	
#	**Phi**	**Theta**
1	0	4.637001
2	0	65.89178
3	4.200798	72.89446
4	115.7992	72.89446
5	120	4.637001
6	120	65.89178
7	124.2008	72.89446
8	235.7992	72.79446
9	240	4.637001
10	240	65.89178
11	244.2008	72.89446
12	355.7992	72.89446

Dimple #	5	
Type	spherical	
Radius	0.075	
SCD	0.008	
TCD	n/a	
#	**Phi**	**Theta**
1	11.39176	35.80355
2	17.86771	45.18952
3	26.35389	29.36327
4	30.46014	74.86406
5	33.84232	84.58637
6	44.16317	84.58634
7	75.83683	84.58634
8	86.15768	84.58637
9	89.53986	74.86406
10	93.64611	29.36327
11	102.1323	45.18952
12	108.6082	35.80355
13	131.3918	35.80355
14	137.8677	45.18952
15	146.3539	29.36327
16	150.4601	74.86406
17	153.8423	84.58637
18	164.1632	84.58634
19	195.8368	84.58634
20	206.1577	84.58637
21	209.5399	74.86406
22	213.6461	29.36327
23	222.1323	45.18952
24	228.6082	35.80355
25	251.3918	35.80355
26	257.8677	45.18952
27	266.3539	29.36327
28	270.4601	74.86406
29	273.8423	84.58637
30	284.1632	84.58634
31	315.8368	84.58634
32	326.1577	84.58637
33	329.5399	74.86406
34	333.6461	29.36327
35	342.1323	45.18952
36	348.6082	35.80355

Dimple #	6	
Type	spherical	
Radius	0.0775	
SCD	0.008	
TCD	n/a	
#	**Phi**	**Theta**
1	22.97427	54.90551
2	27.03771	64.89835
3	47.66575	25.59568
4	54.6796	84.41703
5	65.3204	84.41703
6	72.33425	25.59568
7	92.96229	64.89835
8	97.02573	54.90551
9	142.9743	54.90551
10	147.0377	64.89835
11	167.6657	25.59568
12	174.6796	84.41703
13	185.3204	84.41703
14	192.3343	25.59568
15	212.9623	64.89835
16	217.0257	54.90551
17	262.9743	54.90551
18	267.0377	64.89835
19	287.6657	25.59568
20	294.6796	84.41703
21	305.3204	84.41703
22	312.3343	25.59568
23	332.9623	64.89835
24	337.0257	54.90551

TABLE 8 (Dimple Pattern 174) (continued)

Dimple #	7
Type	spherical
Radius	0.0825
SCD	0.008
TCD	n/a

#	Phi	Theta
1	35.91413	51.35559
2	38.90934	62.34835
3	50.48062	36.43373
4	54.12044	73.49879
5	65.87956	73.49879
6	69.51938	36.43373
7	81.09066	62.34835
8	84.08587	51.35559
9	155.9141	51.35559
10	158.9093	62.34835
11	170.4806	36.43373
12	174.1204	73.49879
13	185.8796	73.49879
14	189.5194	36.43373
15	201.0907	62.34835
16	204.0859	51.35559
17	275.9141	51.35559
18	278.9093	62.34835
19	290.4806	36.43373
20	294.1204	73.49879
21	305.8796	73.49879
22	309.5194	36.43373
23	321.0907	62.34835
24	324.0859	51.35559

Dimple #	8
Type	spherical
Radius	0.0875
SCD	0.008
TCD	n/a

#	Phi	Theta
1	32.46033	39.96433
2	41.97126	73.6516
3	78.02874	73.6516
4	87.53967	39.96433
5	152.4603	39.96433
6	161.9713	73.6516
7	198.0287	73.6516
8	204.5397	39.96433
9	272.4603	39.96433
10	281.9713	73.6516
11	318.0287	73.6516
12	327.5397	39.96433

Dimple #	9
Type	spherical
Radius	0.095
SCD	0.008
TCD	n/a

#	Phi	Theta
1	51.33861	48.5399
2	52.61871	61.45814
3	67.38129	61.45814
4	68.66139	48.53996
5	171.3386	48.53996
6	172.6187	61.45814
7	187.3813	61.45814
8	188.6614	48.53996
9	291.3386	48.53996
10	292.6187	61.45814
11	307.3813	61.45814
12	308.6614	48.53996

TABLE 8 (Dimple Pattern 174) (continued)

Dimple #	1
Type	spherical
Radius	0.05
SCD	0.008
TCD	n/a

#	Phi	Theta
1	0	28.81007
2	0	41.7187
3	5.308533	47.46948
4	9.848338	23.49139
5	17.85912	86.27884
6	22.3436	79.84939
7	24.72264	86.27886
8	95.27736	86.27886
9	97.6564	79.84939
10	102.1409	86.27884
11	110.1517	23.49139
12	114.6915	47.46948
13	120	28.81007
14	120	41.7187
15	125.3085	47.46948
16	129.8483	23.49139
17	137.8591	86.27884
18	142.3436	79.84939
19	144.7226	86.27886
20	215.2774	86.27886
21	217.6564	79.84939
22	222.1409	86.27884
23	230.1517	23.49139
24	234.6915	47.46948
25	240	28.81007
26	240	41.7187
27	245.3085	47.46948
28	249.8483	23.49139
29	257.8591	86.27884
30	262.3436	79.84939
31	264.7226	86.27886
32	335.2774	86.27886
33	337.6564	79.84939
34	342.1409	86.27884
35	350.1517	23.49139
36	354.6915	47.46948

Dimple #	2
Type	spherical
Radius	0.0525
SCD	0.008
TCD	n/a

#	Phi	Theta
1	3.606874	86.10963
2	4.773603	59.66486
3	7.485123	79.72027
4	9.566953	53.68971
5	10.81146	86.10963
6	12.08533	72.79786
7	13.37932	60.13101
8	16.66723	66.70139
9	19.58024	73.34845
10	20.76038	11.6909
11	24.53367	18.8166
12	46.81607	15.97349
13	73.18393	15.97349
14	95.46633	18.8166
15	99.23962	11.6909
16	100.4198	73.34845
17	103.3328	66.70139
18	106.6207	60.13101
19	107.9147	72.79786
20	109.1885	86.10963
21	110.433	53.68971
22	112.5149	79.72027
23	115.2264	59.66486
24	116.3931	86.10963
25	123.6069	86.10963
26	124.7736	59.66486
27	127.4851	79.72027
28	129.567	53.68971
29	130.8115	86.10963
30	132.0853	72.79786
31	133.3793	60.13101
32	136.6672	66.70139
33	139.5802	73.34845
34	140.7604	11.6909
35	144.5337	18.8166
36	166.8161	15.97349
37	193.1839	15.97349
38	215.4663	18.8166
39	219.2396	11.6909
40	220.4198	73.34845
41	223.3328	66.70139
42	226.6207	60.13101
43	227.9147	72.79786
44	229.1885	86.10963
45	230.433	53.68971
46	232.5149	79.72027
47	235.2264	59.66486
48	236.3931	86.10963
49	243.6069	86.10963
50	244.7736	59.66486
51	247.4851	79.72027
52	249.567	53.68971
53	250.8115	86.10963
54	252.0853	72.79786
55	253.3793	60.13101
56	256.6672	66.70139
57	259.5802	73.34845

Dimple #	3
Type	spherical
Radius	0.055
SCD	0.008
TCD	n/a

#	Phi	Theta
1	0	17.13539
2	0	79.62325
3	0	53.39339
4	8.604739	66.19316
5	15.03312	79.65081
6	60	9.094473
7	104.9669	79.65081
8	111.3953	66.19316
9	120	17.13539
10	120	53.39339
11	120	79.62325
12	128.6047	66.19316
13	135.0331	79.65081
14	180	9.094473
15	224.9669	79.65081
16	231.3953	66.19316
17	240	17.13539
18	240	53.39339
19	240	79.62325
20	248.6047	66.19316
21	255.0331	79.65081
22	300	9.094473
23	344.9669	79.65081
24	351.3953	66.19316

TABLE 9 (Dimple Pattern 175)

Dimple #	2 (cont'd)	
#	**Phi**	**Theta**
58	260.7604	11.6909
59	264.5337	18.8166
60	286.8161	15.97349
61	313.1839	15.97349
62	335.4663	18.8166
63	339.2396	11.6909
64	340.4198	73.34845
65	343.3328	66.70139
66	346.6207	60.13101
67	347.9147	72.79786
68	349.1885	86.10963
69	350.433	53.68971
70	352.5149	79.72027
71	355.2264	59.66486
72	356.3931	86.10963

TABLE 9 (Dimple Pattern 175) (continued)

Dimple #	4	
Type	spherical	
Radius	0.0575	
SCD	0.008	
TCD	n/a	
#	**Phi**	**Theta**
1	0	4.637001
2	0	65.89178
3	4.200798	72.89446
4	115.7992	72.89446
5	120	4.637001
6	120	65.89178
7	124.2008	72.89446
8	235.7992	72.89446
9	240	4.637001
10	240	65.89178
11	244.2008	72.89446
12	355.7992	72.89446

Dimple #	5	
Type	truncated	
Radius	0.075	
SCD	0.012	
TCD	0.0035	
#	**Phi**	**Theta**
1	11.39176	35.80355
2	17.86771	45.18952
3	26.35389	29.36327
4	30.46014	74.86406
5	33.84232	84.58637
6	44.16317	84.58634
7	75.83683	84.58634
8	86.15768	84.58637
9	89.53986	74.86406
10	93.64611	29.36327
11	102.1323	45.18952
12	108.6082	35.80355
13	131.3918	35.80355
14	137.8677	45.18952
15	146.3539	29.36327
16	150.4601	74.86406
17	153.8423	84.58637
18	164.1632	84.58634
19	195.8368	84.58634
20	206.1577	84.58637
21	209.5399	74.86406
22	213.6461	29.36327
23	222.1323	45.18952
24	228.6082	35.80355
25	251.3918	35.80355
26	257.8677	45.18952
27	266.3539	29.36327
28	270.4601	74.86406
29	273.8423	84.58637
30	284.1632	84.58634
31	315.8368	84.58634
32	326.1577	84.58637
33	329.5399	74.86406
34	333.6461	29.36327
35	342.1323	45.18952
36	348.6082	35.80355

Dimple #	6	
Type	truncated	
Radius	0.0775	
SCD	0.0122	
TCD	0.0035	
#	**Phi**	**Theta**
1	22.97427	54.90551
2	27.03771	64.89835
3	47.66575	25.59568
4	54.6796	84.41703
5	65.3204	84.41703
6	72.33425	25.59568
7	92.96229	64.89835
8	97.02573	54.90551
9	142.9743	54.90551
10	147.0377	64.89835
11	167.6657	25.59568
12	174.6796	84.41703
13	185.3204	84.41703
14	192.3343	25.59568
15	212.9623	64.89835
16	217.0257	54.90551
17	262.9743	54.90551
18	267.0377	64.89835
19	287.6657	25.59568
20	294.6796	84.41703
21	305.3204	84.41703
22	312.3343	25.59568
23	332.9623	64.89835
24	337.0257	54.90551

TABLE 9 (Dimple Pattern 175) (continued)

Dimple #	7	
Type	truncated	
Radius	0.0825	
SCD	0.0128	
TCD	0.0035	
#	**Phi**	**Theta**
1	35.91413	51.35559
2	38.90934	62.34835
3	50.48062	36.43373
4	54.12044	73.49879
5	65.87956	73.49879
6	69.51938	36.43373
7	81.0966	62.34835
8	84.08587	51.35559
9	155.9141	51.35559
10	158.9093	62.34835
11	170.4806	36.43373
12	174.1204	73.49879
13	185.8796	73.49879
14	189.5194	36.43373
15	201.0907	62.34835
16	204.0859	51.35559
17	275.9141	51.35559
18	278.9093	62.34835
19	290.4806	36.43373
20	294.1204	73.49879
21	305.8796	73.49879
22	309.5194	36.43373
23	321.0907	62.34835
24	324.0859	51.35559

Dimple #	8	
Type	truncated	
Radius	0.0875	
SCD	0.0133	
TCD	0.0035	
#	**Phi**	**Theta**
1	32.46033	39.96433
2	41.97126	73.6516
3	78.02874	73.6516
4	87.53967	39.96433
5	152.4603	39.96433
6	161.9713	73.6516
7	198.0287	73.6516
8	207.5397	39.96433
9	272.4603	39.96433
10	281.9713	73.6516
11	318.0287	73.6516
12	327.5397	39.96433

Dimple #	9	
Type	truncated	
Radius	0.095	
SCD	0.014	
TCD	0.0035	
#	**Phi**	**Theta**
1	51.33861	48.53996
2	52.61871	61.45814
3	67.38129	61.45814
4	68.66139	48.53996
5	171.3386	48.53996
6	172.6187	61.45814
7	187.3813	61.45814
8	188.6614	48.53996
9	291.3386	48.53996
10	292.6187	61.45814
11	307.3813	61.45814
12	308.6614	48.53996

TABLE 9 (Dimple Pattern 175) (continued)

Dimple #	1		**Dimple #**	2		**Dimple #**	3	
Type	truncated		**Type**	truncated		**Type**	truncated	
Radius	0.0750		**Radius**	0.0800		**Radius**	0.0825	
SCD	0.0132		**SCD**	0.0138		**SCD**	0.0141	
TCD	0.0050		**TCD**	0.0050		**TCD**	0.0050	
#	**Phi**	**Theta**	**#**	**Phi**	**Theta**	**#**	**Phi**	**Theta**
1	0	25.85946	1	19.46456	17.6616	1	0	6.707467
2	120	25.85946	2	100.5354	17.6616	2	60	13.5496
3	240	25.85946	3	139.4646	17.6616	3	120	6.707467
4	22.29791	84.58636	4	220.5354	17.6616	4	180	13.5496
5	1.15E-13	44.66932	5	259.4646	17.6616	5	240	6.707467
6	337.7021	84.58636	6	340.5354	17.6616	6	300	13.5496
7	142.2979	84.58636	7	18.02112	74.614	7	6.04096	73.97888
8	120	44.66932	8	7.175662	54.03317	8	13.01903	64.24653
9	457.7021	84.58636	9	352.8243	54.03317	9	2.41E-14	63.82131
10	262.2979	84.58636	10	341.9789	74.614	10	346.981	64.24653
11	240	44.66932	11	348.5695	84.24771	11	353.959	73.97888
12	577.7021	84.58636	12	11.43052	84.24771	12	360	84.07838
			13	138.0211	74.614	13	126.041	73.97888
			14	127.1757	54.03317	14	133.019	64.24653
			15	472.8243	54.03317	15	120	63.82131
			16	461.9789	74.614	16	466.981	64.24653
			17	468.5695	84.24771	17	473.959	73.97888
			18	131.4305	84.24771	18	480	84.07838
			19	258.0211	74.614	19	246.041	73.97888
			20	247.1757	54.03317	20	253.019	64.24653
			21	592.8243	54.03317	21	240	63.82131
			22	581.9789	74.614	22	286.981	64.24653
			23	588.5695	84.24771	23	593.959	73.97888
			24	251.4305	84.24771	24	600	84.07838

TABLE 10 (Dimple Pattern 273)

Dimple #	4	
Type	spherical	
Radius	0.0550	
SCD	0.0075	
TCD	-	
#	Phi	Theta
1	89.81848	78.25196
2	92.38721	71.10446
3	95.11429	63.96444
4	105.6986	42.86305
5	101.558	49.81178
6	98.11364	56.8624
7	100.3784	30.02626
8	86.62335	26.05789
9	69.399	23.82453
10	19.62155	30.02626
11	33.37665	26.05789
12	50.601	23.82453
13	14.30135	42.86305
14	18.44204	49.81178
15	21.88636	56.8624
16	30.18152	78.25196
17	27.61279	71.10446
18	24.88571	63.96444
19	41.03508	85.94042
20	48.61817	85.94042
21	56.20813	85.94042
22	78.96492	85.94042
23	71.38183	85.94042
24	63.79187	85.94042
25	209.8185	78.25196
26	212.3872	71.10446
27	215.1143	63.96444
28	225.6986	42.86305
29	221.558	49.81178
30	218.1136	56.8624
31	220.3784	30.02626
32	206.6234	26.05789
33	189.399	23.82453
34	139.6216	30.02626
35	153.3766	26.05789
36	170.601	23.82453
37	134.3014	42.86305
38	138.442	49.81178
39	141.8864	56.8624
40	150.1815	78.25196
41	147.6128	71.10446
42	144.8857	63.96444
43	161.0351	85.94042
44	168.6182	85.94042
45	176.2081	85.94042
46	198.9649	85.94042
47	191.3818	85.94042
48	183.7919	85.94042
49	329.8185	78.25196
50	332.3872	71.10446
51	336.1143	63.96444
52	345.6986	42.86305
53	341.558	49.81178
54	338.1136	56.8624
55	340.3784	30.02626
56	326.6234	26.05789
57	309.399	23.82453
58	259.6216	30.02626
59	373.3766	26.05789

Dimple #	5	
Type	spherical	
Radius	0.0575	
SCD	0.0075	
TCD	-	
#	Phi	Theta
1	83.35856	69.4858
2	85.57977	61.65549
3	91.04137	46.06539
4	88.0815	53.82973
5	81.86536	34.37733
6	67.54444	32.56834
7	38.13465	34.37733
8	52.45556	32.56834
9	28.95863	46.06539
10	31.9185	53.82973
11	36.64144	69.4858
12	34.42023	61.65549
13	47.55421	77.35324
14	55.84303	77.16119
15	72.44579	77.35324
16	64.15697	77.16119
17	203.3586	69.4858
18	205.5798	61.65549
19	211.0414	46.06539
20	208.0815	53.82973
21	201.8653	34.34433
22	187.5444	32.56834
23	158.1347	34.37733
24	172.4556	32.56834
25	148.9586	46.06539
26	151.9185	63.82973
27	156.6414	69.4858
28	154.4202	61.65549
29	167.5542	77.35324
30	175.843	77.16119
31	192.4458	77.35324
32	184.157	77.16119
33	323.3586	69.4858
34	325.5796	61.65549
35	331.0414	46.06539
36	328.0815	53.82973
37	321.8653	34.37733
38	307.5444	32.56834
39	278.1347	34.37733
40	292.4556	32.56834
41	268.9586	46.06539
42	281.9185	53.82973
43	276.6414	69.4858
44	274.4202	61.65549
45	287.5542	77.35324
46	295.843	77.16119
47	312.4458	77.35324
48	304.157	77.16119

Dimple #	6	
Type	spherical	
Radius	0.0600	
SCD	0.0075	
TCD	-	
#	Phi	Theta
1	86.88247	85.60198
2	110.7202	35.62098
3	9.279821	35.62098
4	33.11753	85.60198
5	206.8825	85.60198
6	230.7202	35.62098
7	129.2798	35.62098
8	153.1175	85.60198
9	326.8825	85.60198
10	350.7202	35.62098
11	249.2798	35.62098
12	273.1175	85.60198

TABLE 10 (Dimple Pattern 273) (continued)

Dimple #	4 (cont'd)	
#	**Phi**	**Theta**
60	290.601	23.82453
61	254.3014	42.86305
62	258.442	49.81178
63	261.8864	56.8624
64	270.1815	78.25196
65	267.6128	71.10446
66	264.8857	63.96444
67	281.0351	85.94042
68	288.6182	85.94042
69	296.2081	85.94042
70	318.9649	85.94042
71	311.3818	85.94042
72	303.7919	85.94042

TABLE 10 (Dimple Pattern 273) (continued)

Dimple #	7		Dimple #	8		Dimple #	9	
Type	spherical		Type	spherical		Type	spherical	
Radius	0.0625		Radius	0.0675		Radius	0.0700	
SCD	0.0075		SCD	0.0075		SCD	0.0075	
TCD	-		TCD	-		TCD	-	
#	Phi	Theta	#	Phi	Theta	#	Phi	Theta
1	80.92949	77.43144	1	74.18416	68.92141	1	65.6084	59.710409
2	76.22245	60.1768	2	79.64177	42.85974	2	66.31567	50.052318
3	77.98598	51.7127	3	40.35823	42.85974	3	53.68433	50.052318
4	94.40845	38.09724	4	45.81584	68.92141	4	54.39516	59.710409
5	66.573	40.85577	5	194.1842	68.92141	5	185.6048	59.710409
6	53.427	40.85577	6	199.6418	42.85974	6	186.3157	50.052318
7	25.59155	38.09724	7	160.3582	42.85974	7	173.6843	50.052318
8	42.01402	51.7127	8	165.8158	68.92141	8	174.3952	59.710409
9	43.77755	60.1768	9	314.1842	68.92141	9	305.6048	59.710409
10	39.07051	77.43144	10	319.6418	42.85974	10	306.3157	50.052318
11	55.39527	68.86469	11	280.3582	42.85974	11	293.6843	50.052318
12	64.60473	68.86469	12	385.8158	68.92141	12	294.3952	59.710409
13	200.9295	77.43144						
14	196.2224	60.1768						
15	197.986	51.7127						
16	214.4085	38.09724						
17	186.573	40.85577						
18	173.427	40.85577						
19	145.5915	38.09724						
20	162.014	61.7127						
21	163.7776	60.1768						
22	159.0705	77.43144						
23	175.3953	68.86469						
24	184.6047	68.86469						
25	320.9295	77.43144						
26	316.2224	60.1768						
27	317.986	51.7127						
28	334.4085	38.09724						
29	306.573	40.85577						
30	293.427	40.85577						
31	265.5915	38.09724						
32	282.014	51.7127						
33	283.7776	60.1768						
34	279.0705	77.43144						
35	295.3953	68.86469						
36	304.6047	68.46469						

TABLE 10 (Dimple Pattern 273) (continued)

Dimple #	1	
Type	spherical	
Radius	0.0550	
SCD	0.0080	
TCD	-	
#	**Phi**	**Theta**
1	89.818	78.252
2	92.387	71.104
3	95.114	63.964
4	105.699	42.863
5	101.558	49.812
6	98.114	56.862
7	100.378	30.026
8	86.623	26.058
9	69.399	23.825
10	19.622	30.026
11	33.377	26.058
12	50.601	23.825
13	14.301	42.863
14	18.442	49.812
15	21.886	56.862
16	30.182	78.252
17	27.613	71.104
18	24.886	63.964
19	41.035	85.940
20	48.618	85.940
21	56.208	85.940
22	78.965	85.940
23	71.382	85.940
24	63.792	85.940
25	209.818	78.252
26	212.387	71.104
27	215.114	63.964
28	225.699	42.863
29	221.558	49.812
30	218.114	56.862
31	220.378	30.026
32	206.623	26.058
33	189.399	30.026
34	139.622	30.026
35	153.377	26.058
36	170.601	23.825
37	134.301	42.863
38	138.442	49.812
39	141.886	56.862
40	150.182	78.252
41	147.613	71.104
42	144.886	63.964
43	161.035	85.940
44	168.618	85.940
45	176.208	85.940
46	198.965	85.940
47	191.382	85.940
48	183.792	85.940
49	329.818	78.252
50	332.387	71.104
51	335.114	63.964
52	345.699	42.863
53	341.558	49.812
54	338.114	56.862
55	340.378	30.026
56	326.623	26.058

Dimple #	2	
Type	spherical	
Radius	0.0575	
SCD	0.0080	
TCD	-	
#	**Phi**	**Theta**
1	83.359	69.486
2	85.500	61.655
3	91.041	46.065
4	88.081	53.830
5	81.865	34.377
6	67.544	32.568
7	38.135	34.377
8	52.456	32.568
9	28.959	46.065
10	31.919	53.830
11	36.641	69.486
12	34.420	61.655
13	47.554	77.353
14	55.843	77.161
15	72.446	77.353
16	64.157	77.161
17	203.359	69.486
18	205.580	61.655
19	211.041	46.065
20	208.081	53.830
21	201.865	34.377
22	187.544	32.568
23	158.135	34.377
24	172.456	32.568
25	148.959	46.065
26	151.919	53.830
27	156.641	69.486
28	154.420	61.655
29	167.544	77.353
30	175.843	77.161
31	192.446	77.353
32	184.157	77.161
33	323.359	69.486
34	325.580	61.655
35	331.041	46.065
36	328.081	53.830
37	321.865	34.377
38	307.544	32.568
39	278.135	34.377
40	292.456	32.568
41	268.959	46.065
42	271.919	53.830
43	276.641	69.486
44	274.420	61.655
45	287.554	77.353
46	295.843	77.161
47	312.446	77.353
48	304.157	77.161

Dimple #	3	
Type	spherical	
Radius	0.0600	
SCD	0.0080	
TCD	-	
#	**Phi**	**Theta**
1	86.882	85.602
2	110.720	35.621
3	9.280	35.621
4	33.118	85.602
5	206.882	85.602
6	230.720	35.621
7	129.280	35.621
8	153.118	85.602
9	326.882	85.602
10	350.720	35.621
11	249.280	35.621
12	273.118	85.602

TABLE 11 (Dimple Pattern 2-3)

57	309.399	23.825
Dimple #	1 (cont'd)	
#	**Phi**	**Theta**
58	259.622	30.026
59	273.377	26.058
60	290.601	23.825
61	254.301	42.863
62	258.442	49.812
63	261.886	56.862
64	270.182	78.252
65	267.613	71.104
66	264.886	63.964
67	281.035	85.940
68	288.618	85.940
69	296.208	85.940
70	318.965	85.940
71	311.382	85.940
72	303.792	85.940

TABLE 11 (Dimple Pattern 2-3) (continued)

Dimple #	4		**Dimple #**	5		**Dimple #**	6	
Type	spherical		**Type**	spherical		**Type**	spherical	
Radius	0.0625		**Radius**	0.0675		**Radius**	0.0700	
SCD	0.0080		**SCD**	0.0080		**SCD**	0.0080	
TCD	-		**TCD**	-		**TCD**	-	
#	**Phi**	**Theta**	**#**	**Phi**	**Theta**	**#**	**Phi**	**Theta**
1	80.929	77.431	1	74.184	68.921	1	65.605	59.710
2	76.222	60.177	2	79.642	42.860	2	66.316	50.052
3	77.986	51.713	3	40.358	42.860	3	53.684	50.052
4	94.408	38.097	4	45.816	68.921	4	54.395	59.710
5	66.573	40.856	5	194.184	68.921	5	185.605	59.710
6	53.427	40.856	6	199.642	42.860	6	186.316	50.052
7	25.592	38.097	7	160.358	42.860	7	173.684	50.052
8	42.014	51.713	8	165.816	68.921	8	174.395	59.710
9	43.778	60.177	9	314.184	68.921	9	305.605	59.710
10	39.071	77.431	10	319.642	42.860	10	306.316	50.052
11	55.395	68.865	11	280.358	42.860	11	293.684	50.052
12	64.605	68.865	12	385.816	68.921	12	294.395	59.710
13	200.929	77.431						
14	196.222	60.177						
15	197.986	51.713						
16	214.408	38.097						
17	186.573	40.856						
18	173.427	40.856						
19	145.592	38.097						
20	162.014	51.713						
21	163.778	60.177						
22	159.071	77.431						
23	175.395	68.865						
24	184.605	68.865						
25	320.929	77.431						
26	316.222	60.177						
27	317.986	51.713						
28	334.408	38.097						
29	306.573	40.856						
30	293.427	40.856						
31	265.592	38.097						
32	282.014	51.713						
33	283.778	60.177						
34	279.071	77.431						
35	295.395	68.865						
36	304.605	68.865						

TABLE 11 (Dimple Pattern 2-3) (continued)

Dimple #	7		Dimple #	8		Dimple #	9	
Type	truncated		**Type**	truncated		**Type**	truncated	
Radius	0.0750		**Radius**	0.0800		**Radius**	0.0825	
SCD	0.0132		**SCD**	0.0138		**SCD**	0.0141	
TCD	0.0055		**TCD**	0.0055		**TCD**	0.0055	
#	**Phi**	**Theta**	**#**	**Phi**	**Theta**	**#**	**Phi**	**Theta**
1	0.000	25.859	1	19.465	17.662	1	0.000	6.707
2	120.000	25.859	2	100.535	17.662	2	60.000	13.550
3	240.000	28.859	3	139.465	17.662	3	120.000	6.707
4	22.298	84.586	4	220.535	17.662	4	180.000	13.550
5	0.000	44.669	5	259.465	17.662	5	240.000	6.707
6	337.702	84.586	6	340.535	17.662	6	300.000	13.550
7	142.298	84.586	7	18.021	74.614	7	6.041	73.979
8	120.000	44.669	8	7.176	54.033	8	13.019	64.247
9	457.702	84.586	9	352.824	54.033	9	0.000	63.821
10	262.298	84.586	10	341.979	74.614	10	346.981	64.247
11	240.000	44.669	11	348.569	84.248	11	353.959	73.979
12	577.702	84.586	12	11.431	84.248	12	360.000	84.078
			13	138.021	74.614	13	126.041	73.979
			14	127.176	54.033	14	133.019	64.247
			15	472.824	54.033	15	120.000	63.821
			16	461.979	74.614	16	466.981	64.247
			17	468.569	84.248	17	473.959	73.979
			18	131.431	84.248	18	480.000	84.078
			19	258.021	74.614	19	246.041	73.979
			20	247.176	54.033	20	253.019	64.247
			21	592.824	54.033	21	240.000	63.821
			22	581.979	74.614	22	586.981	64.247
			23	588.569	84.248	23	593.959	73.979
			24	251.431	84.248	24	600.000	84.078

TABLE 11 (Dimple Pattern 2-3) (continued)

[0082] The geometric and dimple patterns 172-175, 273 and 2-3 described above have been shown to reduce dispersion. Moreover, the geometric and dimple patterns can be selected to achieve lower dispersion based on other ball design parameters as well. For example, for the case of a golf ball that is constructed in such a way as to generate relatively low driver spin, a cuboctahedral dimple pattern with the dimple profiles of the 172-175 series golf balls, shown in Table 5, or the 273 and 2-3 series golf balls shown in Tables 10 and 11, provides for a spherically symmetrical golf ball having less dispersion than other golf balls with similar driver spin rates. This translates into a ball that slices less when struck in such a way that the ball's spin axis corresponds to that of a slice shot. To achieve lower driver spin, a ball can be constructed from e.g., a cover made from an ionomer resin utilizing high-performance ethylene copolymers containing acid groups partially neutralized by using metal salts such as zinc, sodium and others and having a rubber-based core, such as constructed from, for example, a hard Dupont™ Surlyn® covered two-piece ball with a polybutadiene rubber-based core such as the TopFlite XL Straight or a three-piece ball construction with a soft thin cover, e.g., less than about 0.04 inches, with a relatively high flexural modulus mantle layer and with a polybutadiene rubber-based core such as the Titleist ProV1®.

[0083] Similarly, when certain dimple pattern and dimple profiles describe above are used on a ball constructed to generate relatively high driver spin, a spherically symmetrical golf ball that has the short iron control of a higher spinning golf ball and when imparted with a relatively high driver spin causes the golf ball to have a trajectory similar to that of a driver shot trajectory for most lower spinning golf balls and yet will have the control around the green more like a higher spinning golf ball is produced. To achieve higher driver spin, a ball can be constructed from e.g., a soft Dupont™ Surlyn® covered two-piece ball with a hard polybutadiene rubber-based core or a relatively hard Dupont™ Surlyn® covered two-piece ball with a plastic core made of 30-100% DuPont™ HPF 2000®, or a three-piece ball construction with a soft thicker cove, e.g., greater than about 0.04 inches, with a relatively stiff mantle layer and with a polybutadiene rubber-based core.

[0084] It should be appreciated that the dimple patterns and dimple profiles used for 172-175, 273, and 2-3 series golf balls causes these golf balls to generate a lower lift force under various conditions of flight, and reduces the slice dispersion.

[0085] Golf balls dimple patterns 172-175 were subjected to several tests under industry standard laboratory conditions to demonstrate the better performance that the dimple configurations described herein obtain over competing golf balls. In these tests, the flight characteristics and distance performance for golf balls with the 173-175 dimple patterns were conducted and compared with a Titleist Pro V1® made by Acushnet. Also, each of the golf balls with the 172-175 patterns were tested in the Poles-Forward-Backward (PFB) and Pole Horizontal (PH) orientations. The Pro V1® being a USGA conforming ball and thus known to be spherically symmetrical was tested in no particular orientation (random orientation). Golf balls with the 172-175 patterns were all made from basically the same materials and had a standard polybutadiene-based rubber core having 90-105 compression with 45-55 Shore D hardness. The cover was a Surlyn™ blend (38% 9150, 38% 8150, 24% 6320) with a 58-62 Shore D hardness, with an overall ball compression of approximately 110-115.

[0086] The tests were conducted with a "Golf Laboratories" robot and hit with the same Taylor Made® driver at varying club head speeds. The Taylor Made® driver had a 10.5° r7 425 club head with a lie angle of 54 degrees and a REAX 65 'R' shaft. The golf balls were hit in a random-block order, approximately 18-20 shots for each type ball-orientation combination. Further, the balls were tested under conditions to simulate a 20-25 degree slice, e.g., a negative spin axis of 20-25 degrees.

[0087] The testing revealed that the 172-175 dimple patterns produced a ball speed of about 125 miles per hour, while the Pro V1® produced a ball speed of between 127 and 128 miles per hour.

[0088] The data for each ball with patterns 172-175 also indicates that velocity is independent of orientation of the golf balls on the tee.

[0089] The testing also indicated that the 172-175 patterns had a total spin of between 4200 rpm and 4400 rpm, whereas the Pro V1® had a total spin of about 4000 rpm. Thus, the core/cover combination used for balls with the 172-175 patterns produced a slower velocity and higher spinning ball.

[0090] Keeping everything else constant, an increase in a ball's spin rate causes an increase in its lift. Increased lift caused by higher spin would be expected to translate into higher trajectory and greater dispersion than would be expected, e.g., at 200-500 rpm less total spin; however, the testing indicates that the 172-175 patterns have lower maximum trajectory heights than expected. Specifically, the testing revealed that the 172-175 series of balls achieve a max height of about 21 yards, while the Pro V1 ® is closer to 25 yards.

[0091] The data for each of golf balls with the 172-175 patterns indicated that total spin and max height was independent of orientation, which further indicates that the 172-175 series golf balls were spherically symmetrical.

[0092] Despite the higher spin rate of a golf ball with, e.g., pattern 173, it had a significantly lower maximum trajectory height (max height) than the Pro V1®. Of course, higher velocity will result in a higher ball flight. Thus, one would expect the Pro V1® to achieve a higher max height, since it had a higher velocity. If a core/cover combination had been used for the 172-175 series of golf balls that produced velocities in the range of that achieved by the Pro V1®, then one would expect a higher max height. But the fact that the max height was so low for the 172-175 series of golf balls despite the higher total spin suggests that the 172-175 Vballs would still not achieve as high a max height as the Pro V1® even if the initial velocities for the 172-175 series of golf balls were 2-3 mph higher.

[0093] Figure 11 is a graph of the maximum trajectory height (Max Height) versus initial total spin rate for all of the 172-175 series golf balls and the Pro V1 ®. These balls were when hit with Golf Labs robot using a 10.5 degree Taylor Made r7 425 driver with a club head speed of approximately 90 mph imparting an approximately 20 degree spin axis slice. As can be seen, the 172-175 series of golf balls had max heights of between 18-24 yards over a range of initial total spin rates of between about 3700 rpm and 4100 rpm, while the Pro V1® had a max height of between about 23.5 and 26 yards over the same range.

[0094] The maximum trajectory height data correlates directly with the CL produced by each golf ball. These results indicate that the Pro V1 ® golf ball generated more lift than any of the 172-175 series balls. Further, some of balls with the 172-175 patterns climb more slowly to the maximum trajectory height during flight, indicating they have a slightly lower lift exerted over a longer time period. In operation, a golf ball with the 173 pattern exhibits lower maximum trajectory height than the leading comparison golf balls for the same spin, as the dimple profile of the dimples in the square and triangular regions of the cuboctahedral pattern on the surface of the golf ball cause the air layer to be manipulated differently during flight of the golf ball.

[0095] Despite having higher spin rates, the 172-175 series golf balls have Carry Dispersions that are on average less than that of the Pro V1® golf ball. The data in figures 12-16 clearly shows that the 172-175 series golf balls have Carry Dispersions that are on average less than that of the Pro V1® golf ball. It should be noted that the 172-175 series of balls are spherically symmetrical and conform to the USGA Rules of Golf.

[0096] Figure 12 is a graph illustrating the carry dispersion for the balls tested and shown in Figure 11. As can be seen, the average carry dispersion for the 172-175 balls is between 50-60 ft, whereas it is over 60 feet for the Pro V1®.

[0097] Figure 13-16 are graphs of the Carry Dispersion versus Total Spin rate for the 172-175 golf balls versus the Pro V1®. The graphs illustrate that for each of the balls with the 172-175 patterns and for a given spin rate, the balls with the 172-175 patterns have a lower Carry Dispersion than the Pro V1®. For example, for a given spin rate, a ball with the 173 pattern appears to have 10-12 ft lower carry dispersion than the Pro V1® golf ball. In fact, a 173 golf ball had the lowest dispersion performance on average of the 172-175 series of golf balls.

[0098] The overall performance of the 173 golf ball as compared to the Pro V1® golf ball is illustrated in figures 17 and 18. The data in these figures shows that the 173 golf ball has lower lift than the Pro V1® golf ball over the same range of Dimensionless Spin Parameter (DSP) and Reynolds Numbers.

[0099] Figure 17 is a graph of the wind tunnel testing results showing of the Lift Coefficient (CL) versus DSP for the 173 golf ball against different Reynolds Numbers. The DSP values are in the range of 0.0 to 0.4. The wind tunnel testing was performed using a spindle of $1/16^{th}$ inch in diameter.

[00100] Figure 18 is a graph of the wind tunnel test results showing the CL versus DSP for the Pro V1 golf ball against different Reynolds Numbers.

[00101] In operation and as illustrated in figures 17 and 18, for a DSP of 0.20 and a Re of greater than about 60,000, the CL for the 173 golf ball is approximately 0.19-0.21, whereas for the Pro V1® golf ball under the same DSP and Re conditions, the CL is about .25-.27. On a percentage basis, the 173 golf ball is generating about 20-25% less lift than the Pro V1® golf ball. Also, as the Reynolds Number drops down to the 60,000 range, the difference in CL is pronounced – the Pro V1® golf ball lift remains positive while the 173 golf ball becomes negative. Over the entire range of DSP and Reynolds Numbers, the 173 golf ball has a lower lift coefficient at a given DSP and Reynolds pair than does the Pro V1® golf ball. Furthermore, the DSP for the 173 golf ball has to rise from 0.2 to more than 0.3 before CL is equal to that of CL for the Pro V1® golf ball. Therefore, the 173 golf ball performs better than the Pro V1® golf ball in terms of lift-induced dispersion (non-zero spin axis).

[00102] Therefore, it should be appreciated that the cuboctahedron dimple pattern on the 173 golf ball with large truncated dimples in the square sections and small spherical dimples in the triangular sections exhibits low lift for normal driver spin

and velocity conditions. The lower lift of the 173 golf ball translates directly into lower dispersion and, thus, more accuracy for slice shots.

[00103] "Premium category" golf balls like the Pro V1® golf ball often use a three-piece construction to reduce the spin rate for driver shots so that the ball has a longer distance yet still has good spin from the short irons. The 173 dimple pattern can cause the golf ball to exhibit relatively low lift even at relatively high spin conditions. Using the low-lift dimple pattern of the 173 golf ball on a higher spinning two-piece ball results in a two-piece ball that performs nearly as well on short iron shots as the "premium category" golf balls currently being used.

[00104] The 173 golf ball's better distance-spin performance has important implications for ball design in that a ball with a higher spin off the driver will not sacrifice as much distance loss using a low-lift dimple pattern like that of the 173 golf ball. Thus the 173 dimple pattern or ones with similar low-lift can be used on higher spinning and less expensive two-piece golf balls that have higher spin off a PW but also have higher spin off a driver. A two-piece golf ball construction in general uses less expensive materials, is less expensive, and easier to manufacture. The same idea of using the 173 dimple pattern on a higher spinning golf ball can also be applied to a higher spinning one-piece golf ball.

[00105] Golf balls like the MC Lady and MaxFli Noodle use a soft core (approximately 50-70 PGA compression) and a soft cover (approximately 48-60 Shore D) to achieve a golf ball with fairly good driver distance and reasonable spin off the short irons. Placing a low-lift dimple pattern on these balls allows the core hardness to be raised while still keeping the cover hardness relatively low. A ball with this design

has increased velocity, increased driver spin rate, and is easier to manufacture; the low-lift dimple pattern lessens several of the negative effects of the higher spin rate.

[00106] The 172-175 dimple patterns provide the advantage of a higher spin two-piece construction ball as well as being spherically symmetrical. Accordingly, the 172-175 series of golf balls perform essentially the same regardless of orientation.

[00107] In an alternate embodiment, a non-Conforming Distance Ball having a thermoplastic core and using the low-lift dimple pattern, e.g., the 173 pattern, can be provided. In this alternate embodiment golf ball, a core, e.g., made with DuPont™ Surlyn® HPF 2000 is used in a two- or multi-piece golf ball. The HPF 2000 gives a core with a very high COR and this directly translates into a very fast initial ball velocity – higher than allowed by the USGA regulations.

[00108] In yet another embodiment, as shown in figure 19, golf ball 600 is provided having a spherically symmetrical low-lift pattern that has two types of regions with distinctly different dimples. As one non-limiting example of the dimple pattern used for golf ball 600, the surface of golf ball 600 is arranged in an octahedron pattern having eight symmetrical triangular shaped regions 602, which contain substantially the same types of dimples. The eight regions 602 are created by encircling golf ball 600 with three orthogonal great circles 604, 606 and 608 and the eight regions 602 are bordered by the intersecting great circles 604, 606 and 608. If dimples were placed on each side of the orthogonal great circles 604, 606 and 608, these “great circle dimples” would then define one type of dimple region two dimples wide and the other type region would be defined by the areas between the great circle dimples. Therefore, the dimple pattern in the octahedron design would have two distinct dimple areas created by placing one type of dimple in the great circle regions 604, 606 and 608 and a second

type dimple in the eight regions 602 defined by the area between the great circles 604, 606 and 608.

[00109] As can be seen in figure 19, the dimples in the region defined by circles 604, 606, and 608 can be truncated dimples, while the dimples in the triangular regions 602 can be spherical dimples. In other embodiments, the dimple type can be reversed. Further, the radius of the dimples in the two regions can be substantially similar or can vary relative to each other.

[00110] Figures 25 and 26 are graphs which were generated for balls 273 and 2-3 in a similar manner to the graphs illustrated in Figures 20 to 24 for some known balls and the 173 and 273 balls. Figures 25 and 26 show the lift coefficient versus Reynolds Number at initial spin rates of 4,000 rpm and 4,500 rpm, respectively, for the 273 and 2-3 dimple pattern. Figures 27 and 28 are graphs illustrating the drag coefficient versus Reynolds number at initial spin rates of 4000 rpm and 4500 rpm, respectively, for the 273 and 2-3 dimple pattern. Figures 25 to 28 compare the lift and drag performance of the 273 and 2-3 dimple patterns over a range of 120,000 to 140,000 Re and for 4000 and 4500 rpm. This illustrates that balls with dimple pattern 2-3 perform better than balls with dimple pattern 273. Balls with dimple pattern 2-3 were found to have the lowest lift and drag of all the ball designs which were tested.

[00111] While certain embodiments have been described above, it will be understood that the embodiments described are by way of example only. Accordingly, the systems and methods described herein should not be limited based on the described embodiments. Rather, the systems and methods described herein should only be limited in light of the claims that follow when taken in conjunction with the above description and accompanying drawings.

What is claimed is:

1. A golf ball having a plurality of dimples formed on its outer surface, the outer surface of the golf ball being divided into first and second areas each containing a plurality of dimples, the first and second areas being of different shapes, each first area containing first dimples and each second area containing second dimples, at least some first dimples being of different types from the second dimples, and the first areas being formed of circular paths around the outer surface of the ball, the second areas being formed by the intersection of the circular paths.

2. The golf ball of claim 1, wherein the circular paths extend along substantially geodesic lines.

3. The golf ball of claim 2, wherein the circular paths define plural first areas comprising at least two orthogonal, intersecting geodesic paths, and plural second areas defined between the intersecting geodesic paths.

4. The golf ball of claim 3, wherein the first areas comprise three intersecting, orthogonal geodesic paths and the second areas comprise eight triangular areas defining a substantially octahedral pattern.

5. The golf ball of claim 4, wherein the total number of second dimples is greater than the total number of first dimples.

6. The golf ball of claim 2, wherein each geodesic path contains at least one row of dimples extending around the circumference of the ball.

7. The golf ball of claim 2, wherein each geodesic path contains two side-by-side rows of dimples extending around the circumference of the ball.

8. The golf ball of claim 3, wherein the first dimples are larger than the second dimples.

9. The golf ball of claim 3, wherein the first dimples are smaller than the second dimples.

10. The golf ball of claim 1, wherein the first and second areas each contain dimples of at least two different sizes.

11. The golf ball of claim 1, wherein the areas define a generally octahedron pattern on the outer surface of the golf ball.

12. The golf ball of claim 1, wherein the first dimples are of different diameter from the second dimples.

13. The golf ball of claim 1, wherein the first dimples are of different chord depth from the second dimples.

14. The golf ball of claim 1, wherein the first and second dimples are of different chord depths and diameters.

15. The golf ball of claim 1, wherein at least one of the first and second areas contains dimples of at least two different sizes.

16. The golf ball of claim 1, wherein the first dimples are of smaller diameter than the second dimples.

17. The golf ball of claim 16, wherein the first dimples are of deeper chord depth than the second dimples.

18. The golf ball of claim 16, wherein the first dimples are of shallower chord depth than the second dimples.

19. The golf ball of claim 1, wherein the outer surface is divided into eleven areas of dimples.

20. The golf ball of claim 1, wherein the first dimples are spherical truncated dimples having flat inner ends and the second dimples are spherical dimples.

21. The golf ball of claim 20, wherein the first areas are intersecting, orthogonal geodesic paths and the second areas are triangular.

22. The golf ball of claim 20, wherein the first dimples have a first, truncated chord depth which is less than the chord depth of the second dimples.

23. The golf ball of claim 22, wherein the second dimples have a larger radius than the first dimples.

24. The golf ball of claim 21, wherein there are twenty one second dimples in each triangular area.

25. The golf ball of claim 20, wherein the first dimples are all of the same radius and chord depth.

26. The golf ball of claim 20, wherein the second dimples are all of the same radius and chord depth.

27. The golf ball of claim 1, wherein the first dimples being of different dimensions from the second dimples such that the first and second groups of areas are visually contrasting.

28. The golf ball of claim 1, wherein the first and second areas produce different aero-dynamic effects.

29. The golf ball of claim 1, wherein the first dimples have a different average diameter compared to the second dimples.

30. The golf ball of claim 1, wherein the first dimples are spherical dimples having flat inner ends and the second dimples are spherical truncated dimples.

31. The golf ball of claim 1, wherein some of the dimples are formed from a lattice structure.

32. The golf ball of claim 1, wherein the average volume per dimple is greater in one of the groups of areas relative to the other.

33. The golf ball of claim 1, wherein the unit volume in one area is greater than in the other area, and wherein unit volume is defined as the volume of the dimples in the area divided by the surface area in that area.

34. The golf ball of claim 1, wherein the unit volume in one area is at least 5% greater than in the other area, and wherein unit volume is defined as the volume of the dimples in the area divided by the surface area in that area.

35. The golf ball of claim 1, wherein the unit volume in one area is at least 15% greater than in the other area, and wherein unit volume is defined as the volume of the dimples in the area divided by the surface area in that area.

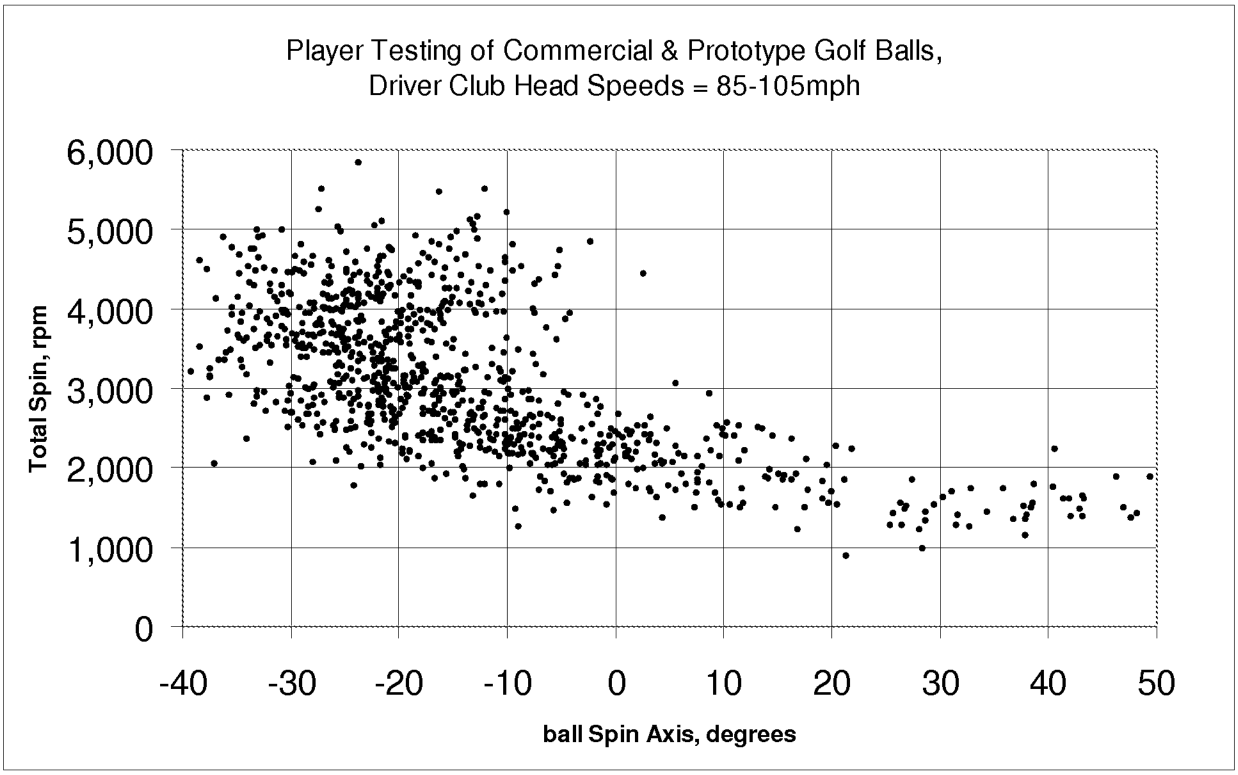
Player Testing of Commercial & Prototype Golf Balls,
Driver Club Head Speeds = 85-105mph
Total Spin, rpm
6,000
5,000
4,000
3,000
2,000
1,000
0
-40
-30
-20
-10
0
10
20
30
40
50
ball Spin Axis, degrees

FIG. 1

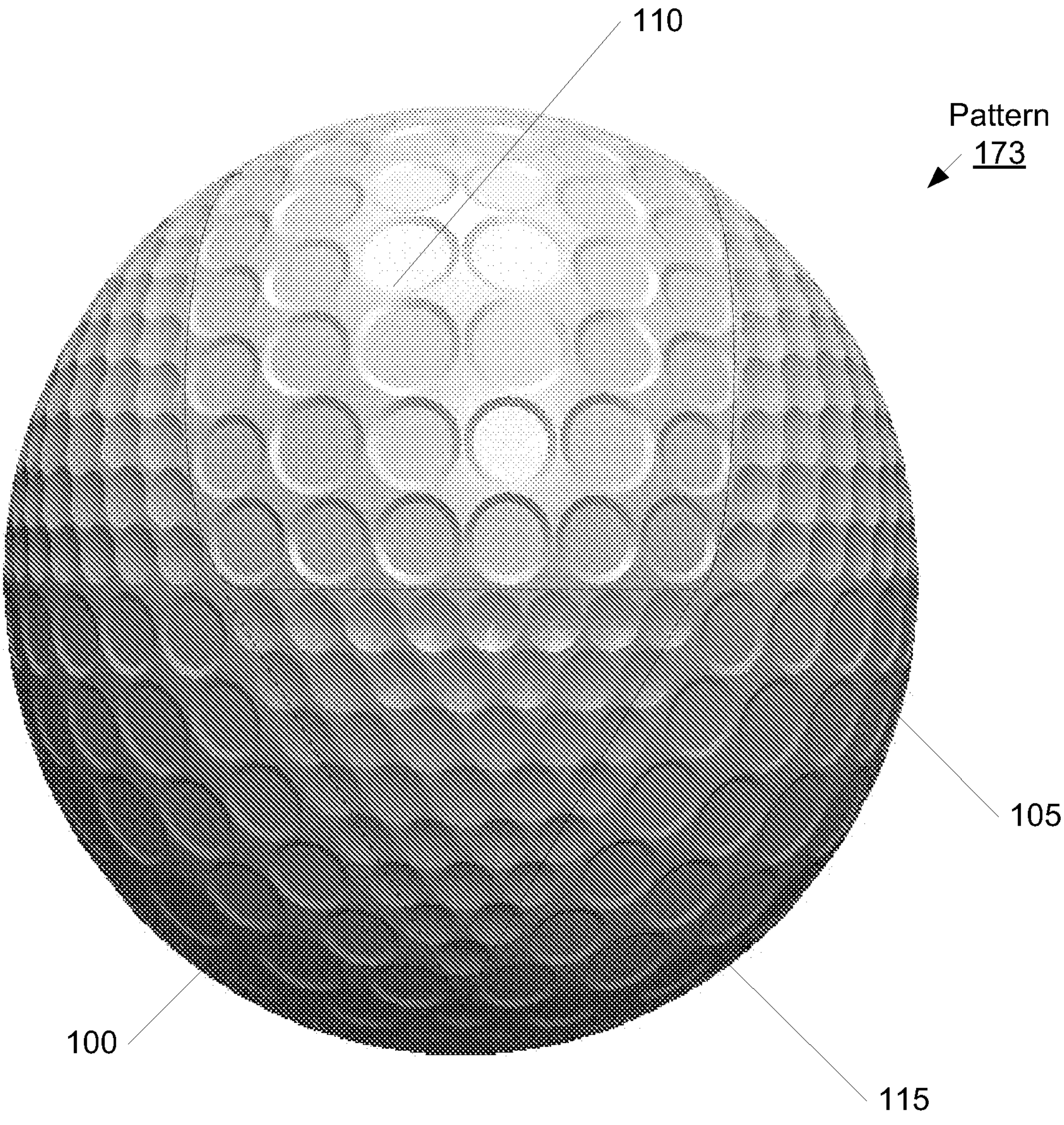

FIG. 2

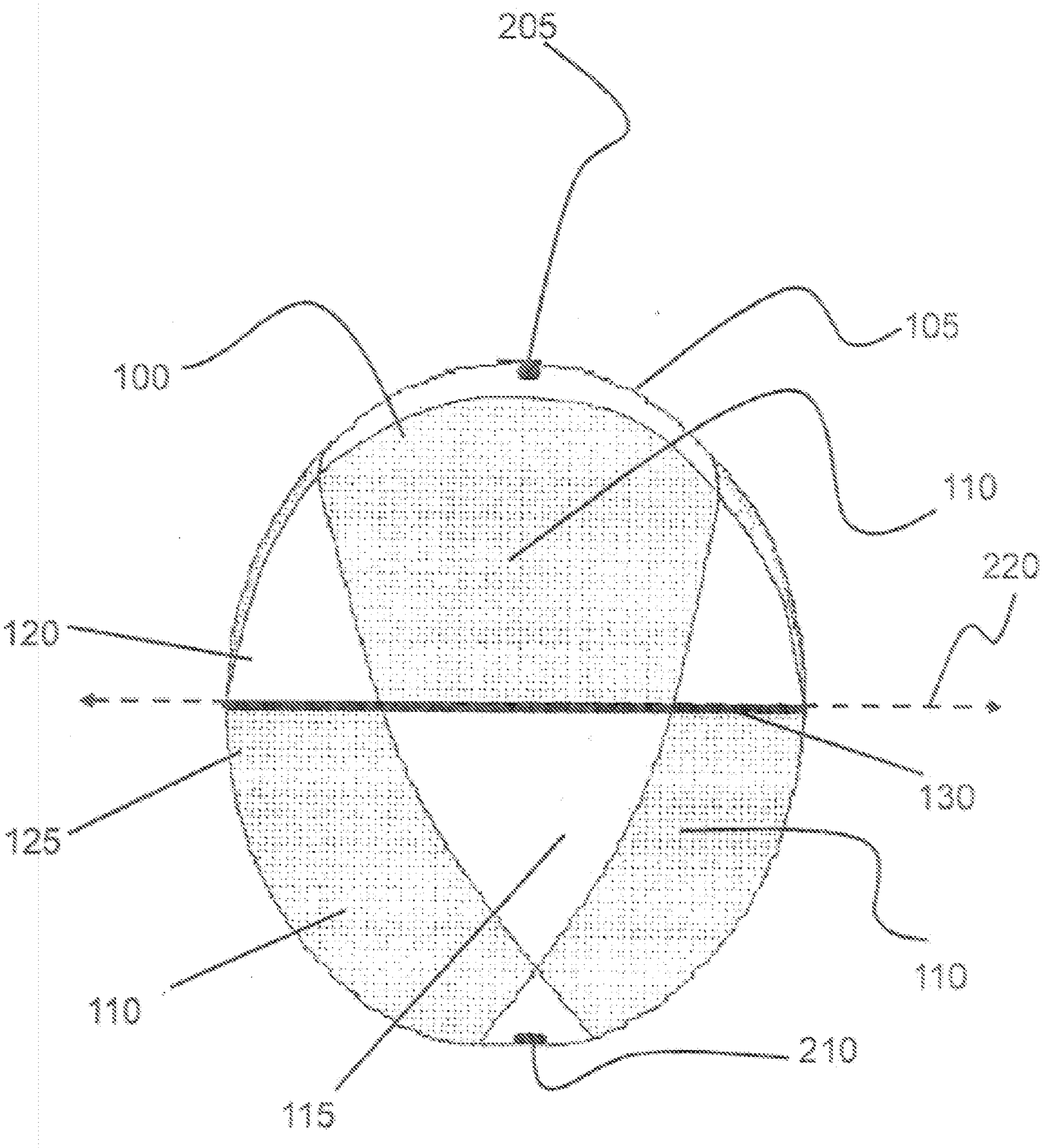

FIG. 3

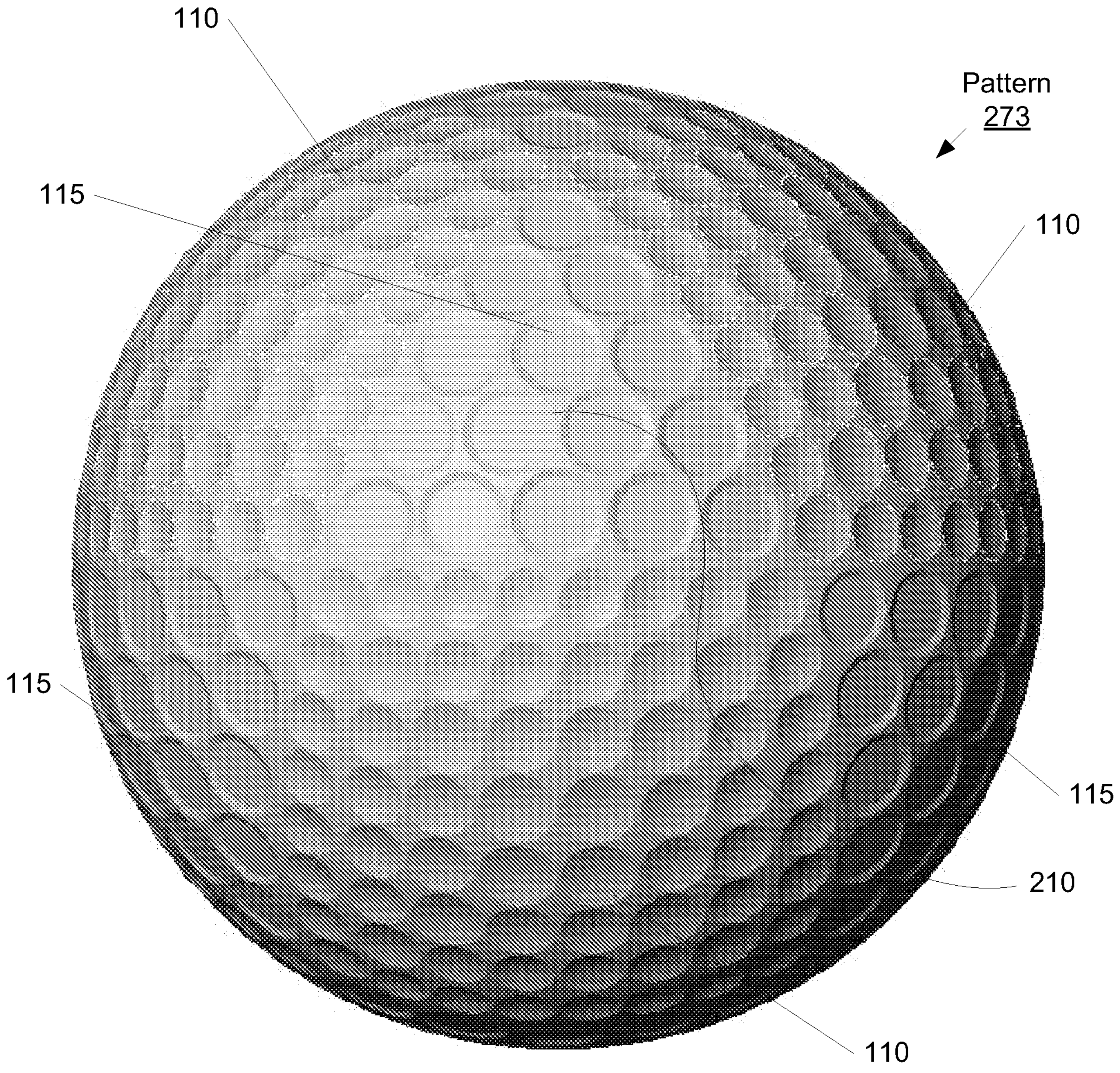

FIG. 4

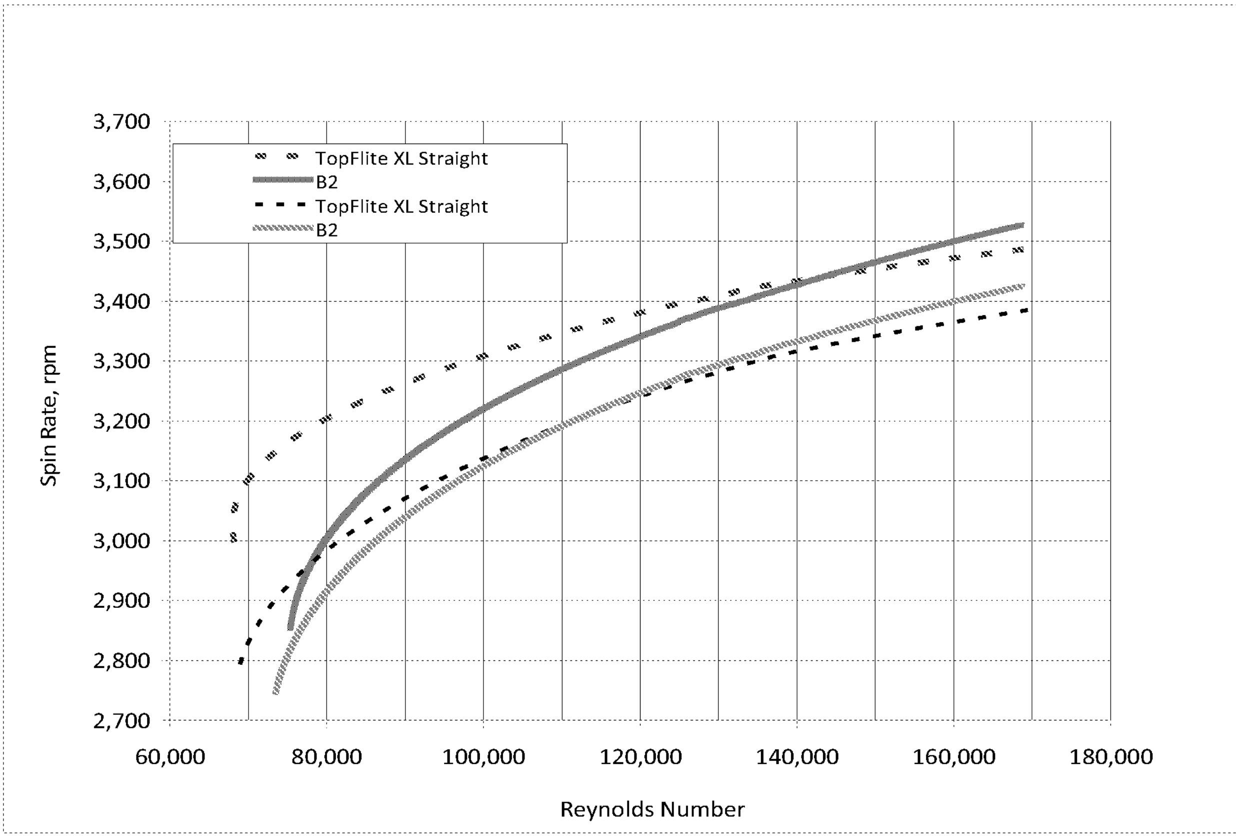
TopFlite XL Straight
B2
TopFlite XL Straight
B2
3,700
3,600
3,500
3,400
3,300
3,200
3,100
3,000
2,900
2,800
2,700
Spin Rate, rpm
60,000
80,000
100,000
120,000
140,000
160,000
180,000
Reynolds Number

FIG. 5

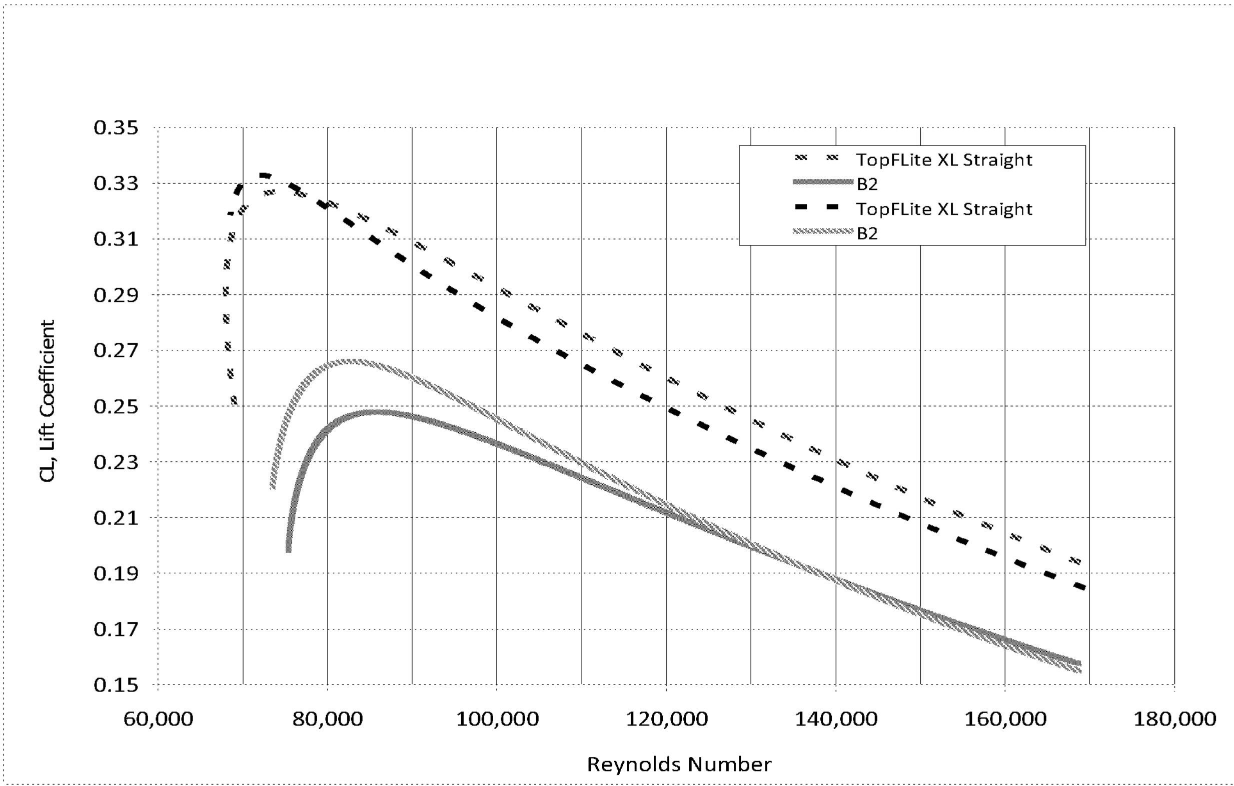
TopFLite XL Straight
B2
TopFLite XL Straight
B2
0.35
0.33
0.31
0.29
0.27
0.25
0.23
0.21
0.19
0.17
0.15
CL, Lift Coefficient
60,000
80,000
100,000
120,000
140,000
160,000
180,000
Reynolds Number

FIG. 6

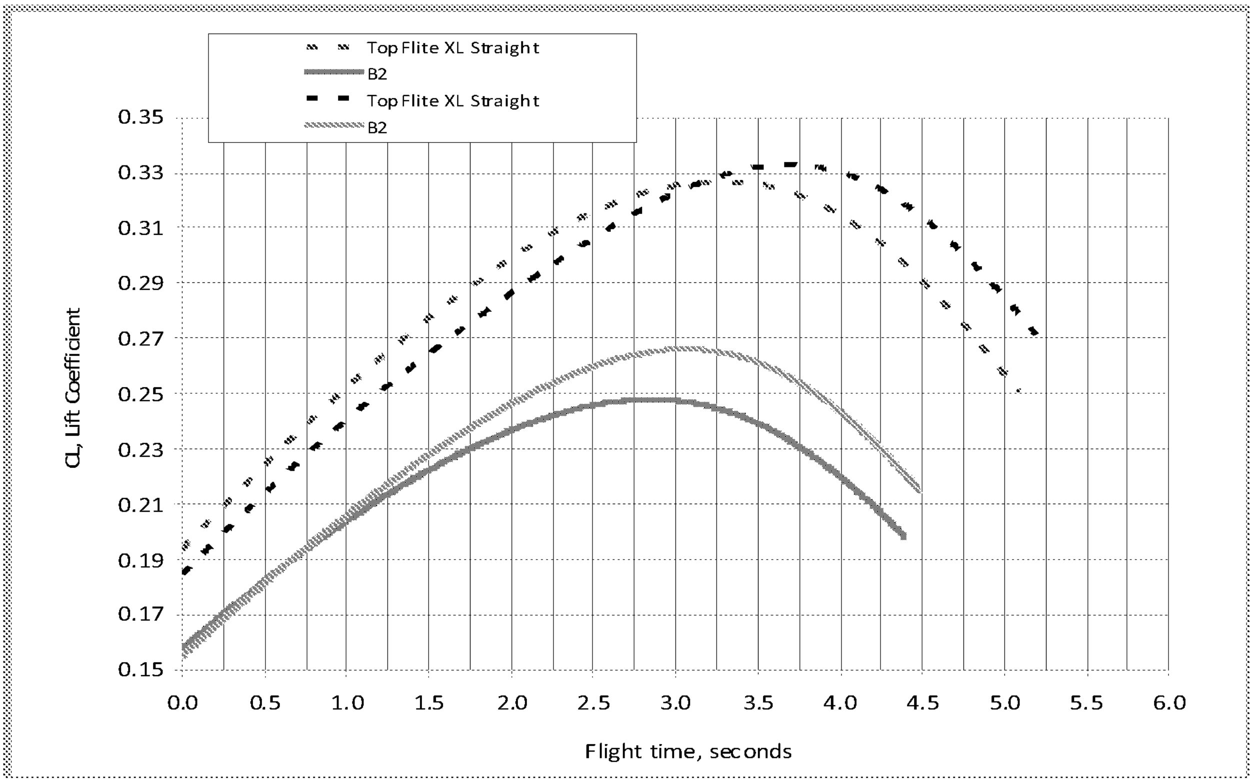
Top Flite XL Straight
B2
Top Flite XL Straight
B2
0.35
0.33
0.31
0.29
0.27
0.25
0.23
0.21
0.19
0.17
0.15
CL, Lift Coefficient
0.0
0.5
1.0
1.5
2.0
2.5
3.0
3.5
4.0
4.5
5.0
5.5
6.0
Flight time, seconds

FIG. 7

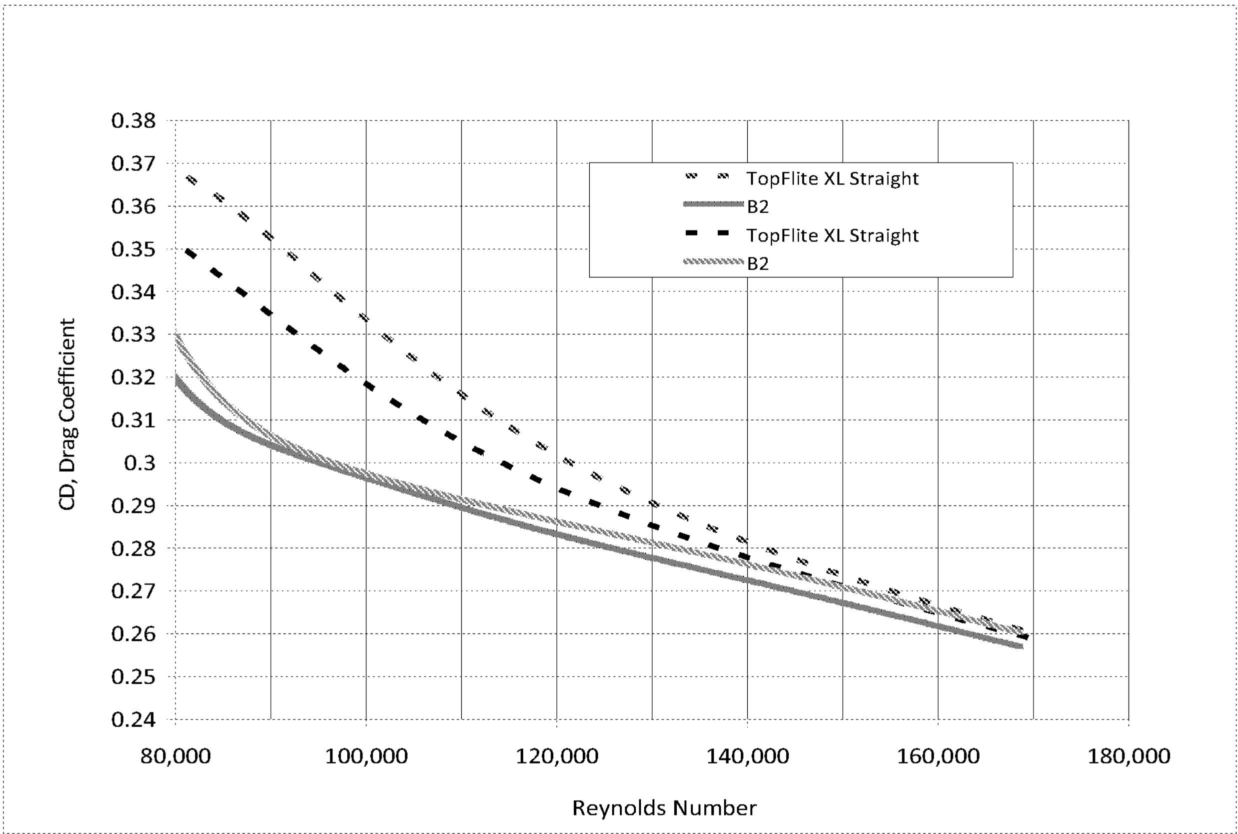
0.38
0.37
0.36
0.35
0.34
0.33
0.32
0.31
0.3
0.29
0.28
0.27
0.26
0.25
0.24
CD, Drag Coefficient
TopFlite XL Straight
B2
TopFlite XL Straight
B2
80,000
100,000
120,000
140,000
160,000
180,000
Reynolds Number

FIG. 8

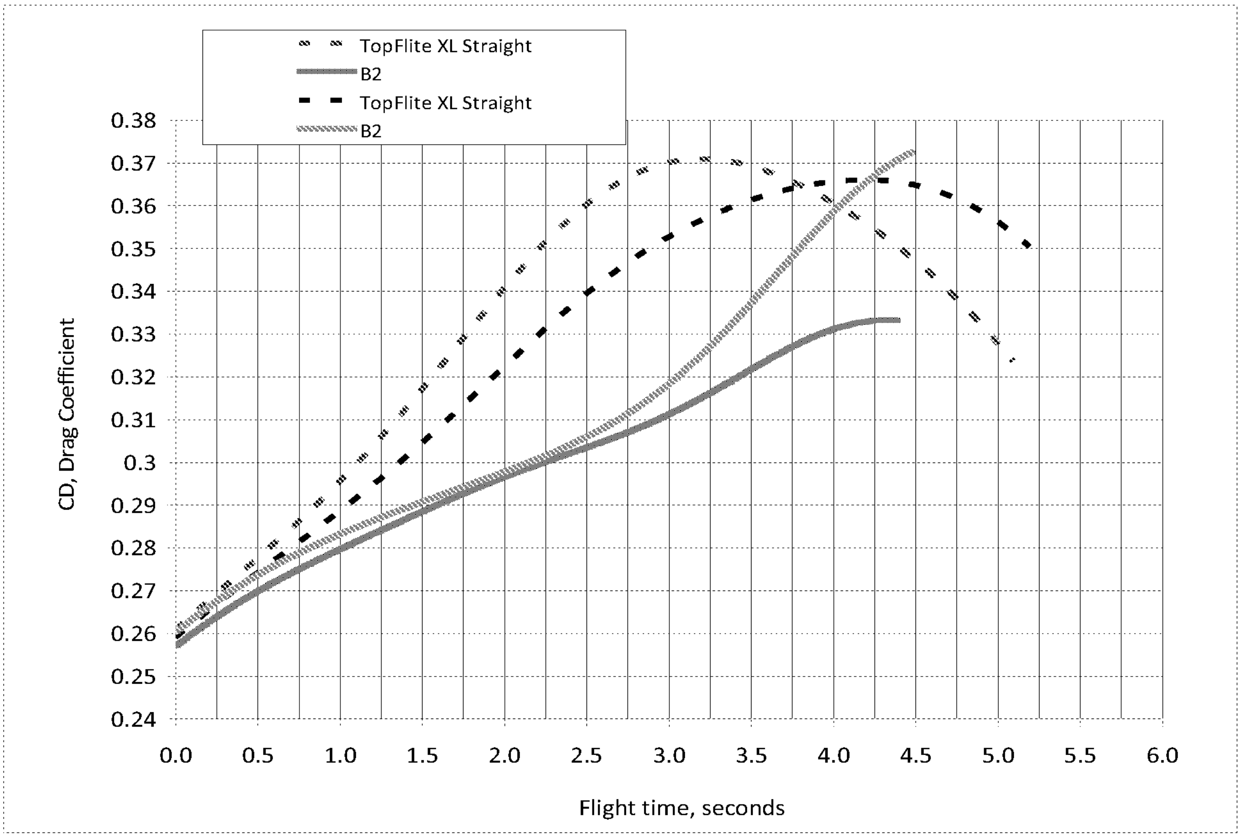
TopFlite XL Straight
B2
TopFlite XL Straight
B2
0.38
0.37
0.36
0.35
0.34
0.33
0.32
0.31
0.3
0.29
0.28
0.27
0.26
0.25
0.24
CD, Drag Coefficient
0.0
0.5
1.0
1.5
2.0
2.5
3.0
3.5
4.0
4.5
5.0
5.5
6.0
Flight time, seconds

FIG. 9

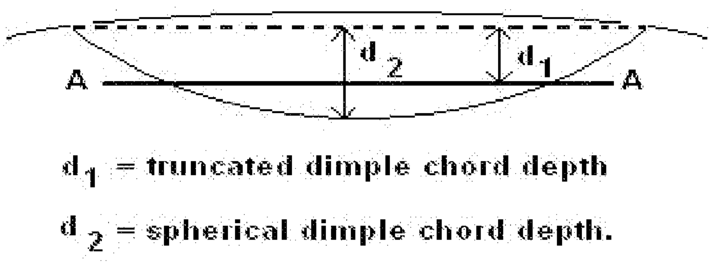
d 2
d 1
A
A
d 1 = truncated dimple chord depth
d 2 = spherical dimple chord depth.

FIG. 10

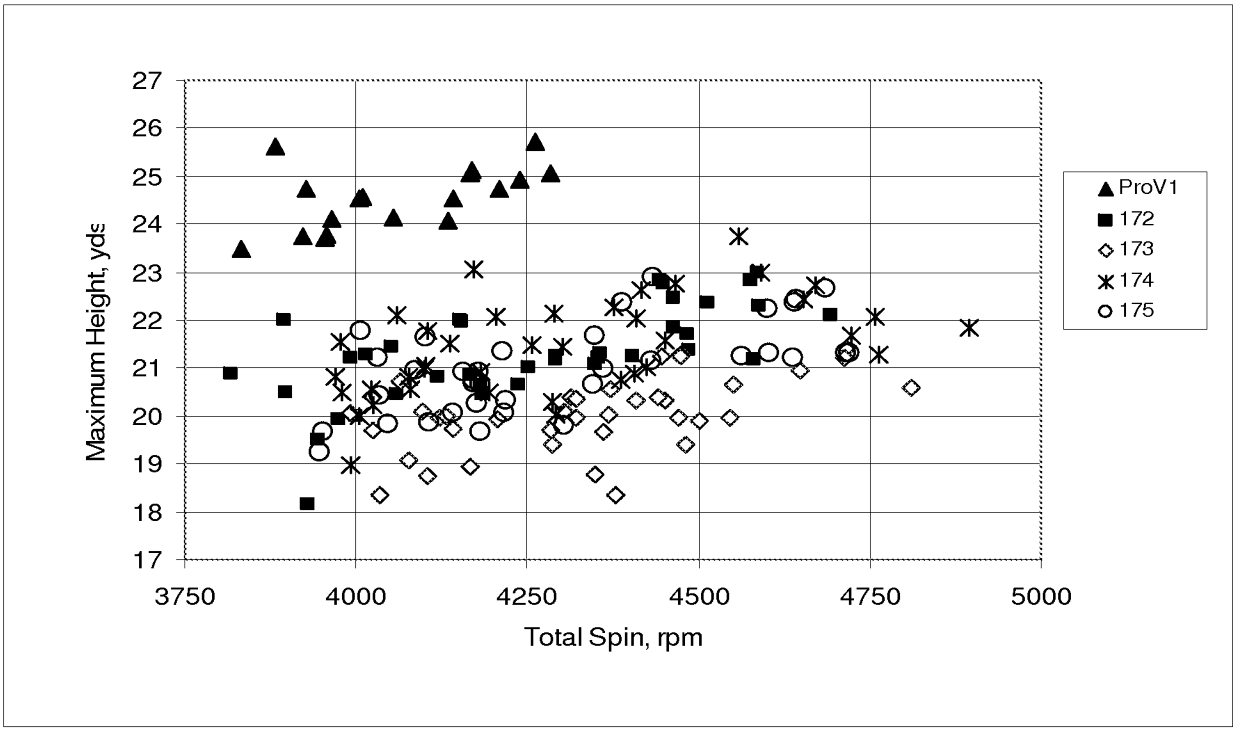

Maximum Height, yds
27
26
25
24
23
22
21
20
19
18
17
3750
4000
4250
4500
4750
5000
Total Spin, rpm
ProV1
172
173
174
175

FIG. 11

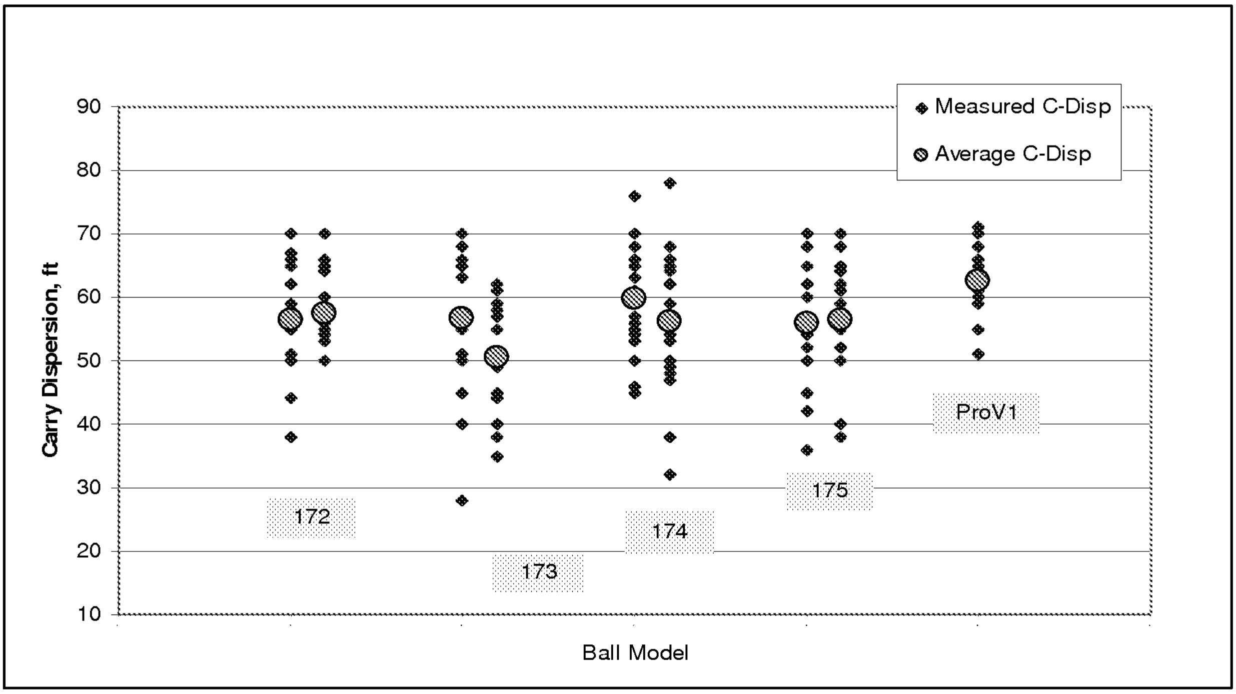
Measured C-Disp
Average C-Disp
Carry Dispersion, ft
90
80
70
60
50
40
30
20
10
172
173
174
175
ProV1
Ball Model

FIG. 12

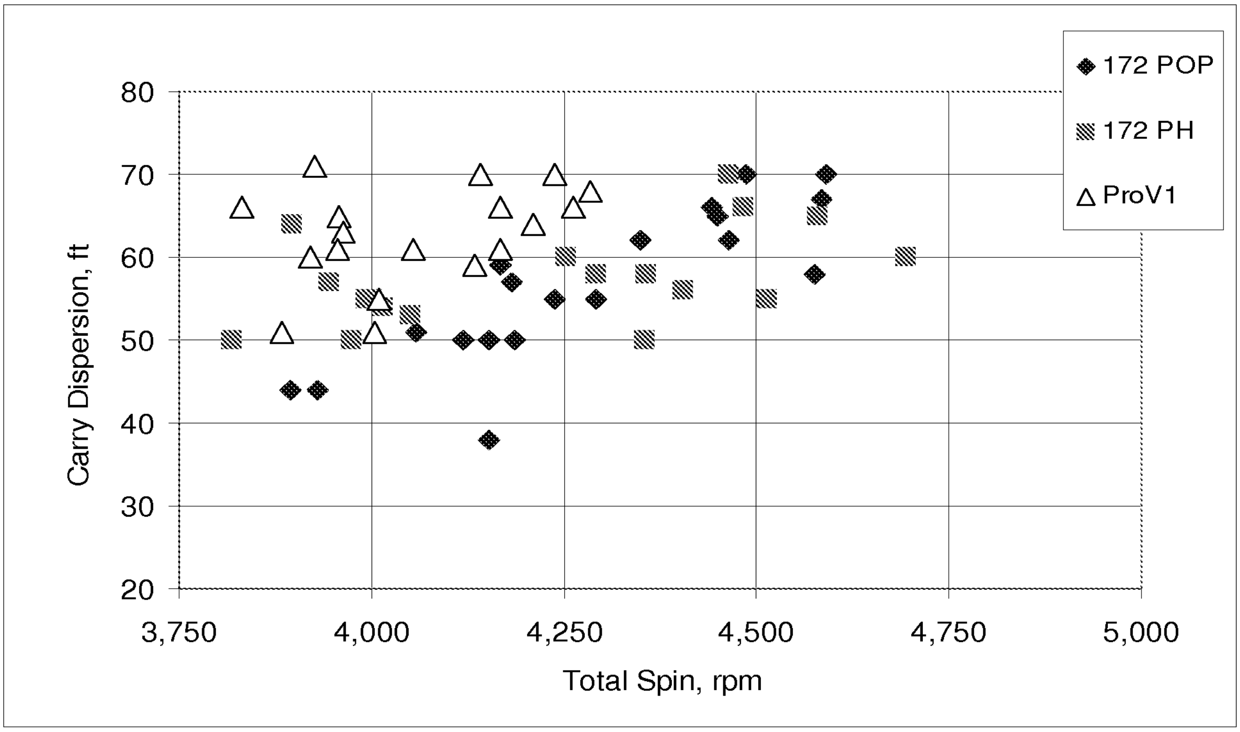
172 POP
172 PH
ProV1
Carry Dispersion, ft
80
70
60
50
40
30
20
3,750
4,000
4,250
4,500
4,750
5,000
Total Spin, rpm

FIG. 13

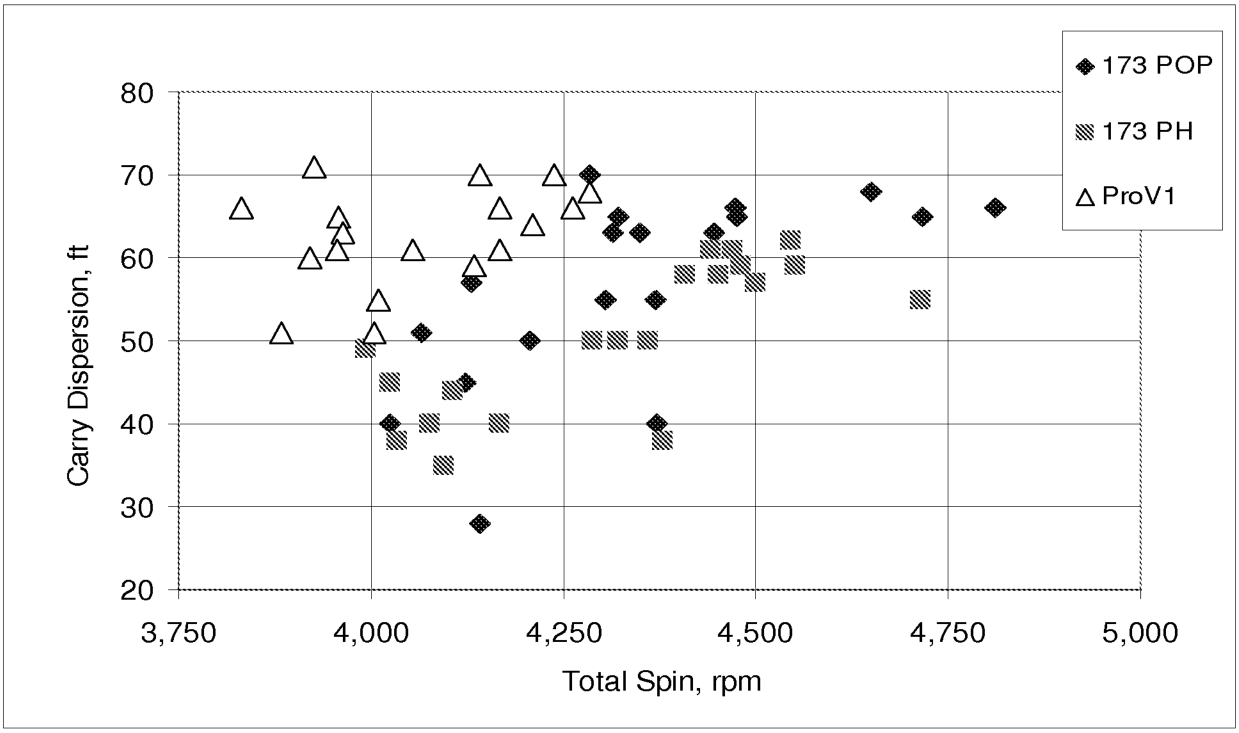
80
70
60
50
40
30
20
Carry Dispersion, ft
3,750
4,000
4,250
4,500
4,750
5,000
Total Spin, rpm
173 POP
173 PH
ProV1

FIG. 14

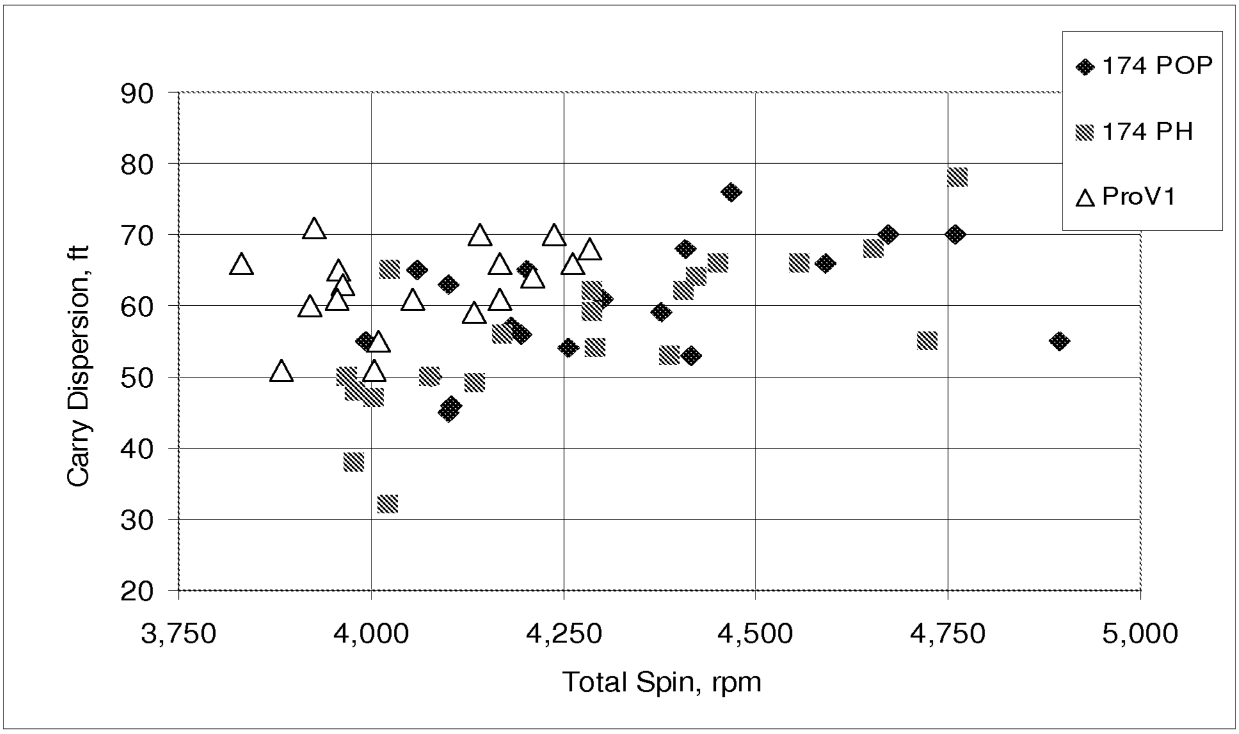
174 POP
174 PH
ProV1
90
80
70
60
50
40
30
20
Carry Dispersion, ft
3,750
4,000
4,250
4,500
4,750
5,000
Total Spin, rpm

FIG. 15

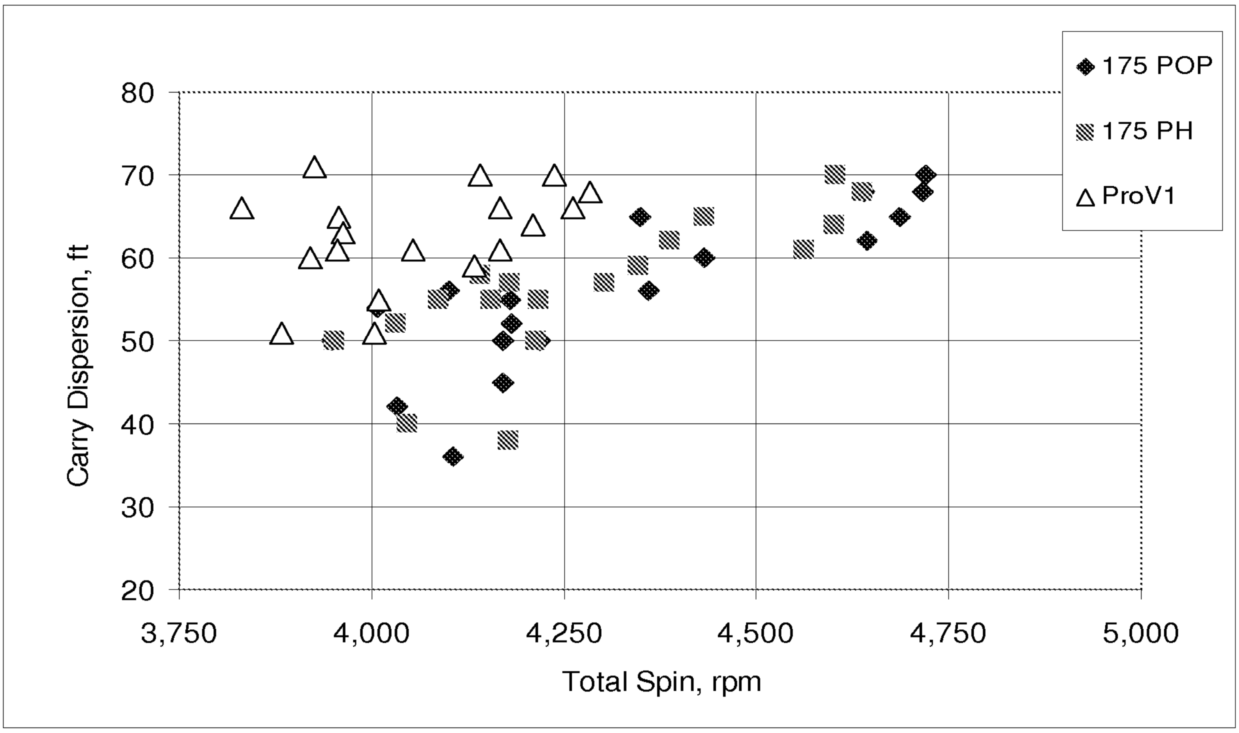
80
70
60
50
40
30
20
Carry Dispersion, ft
3,750
4,000
4,250
4,500
4,750
5,000
Total Spin, rpm
175 POP
175 PH
ProV1

FIG. 16

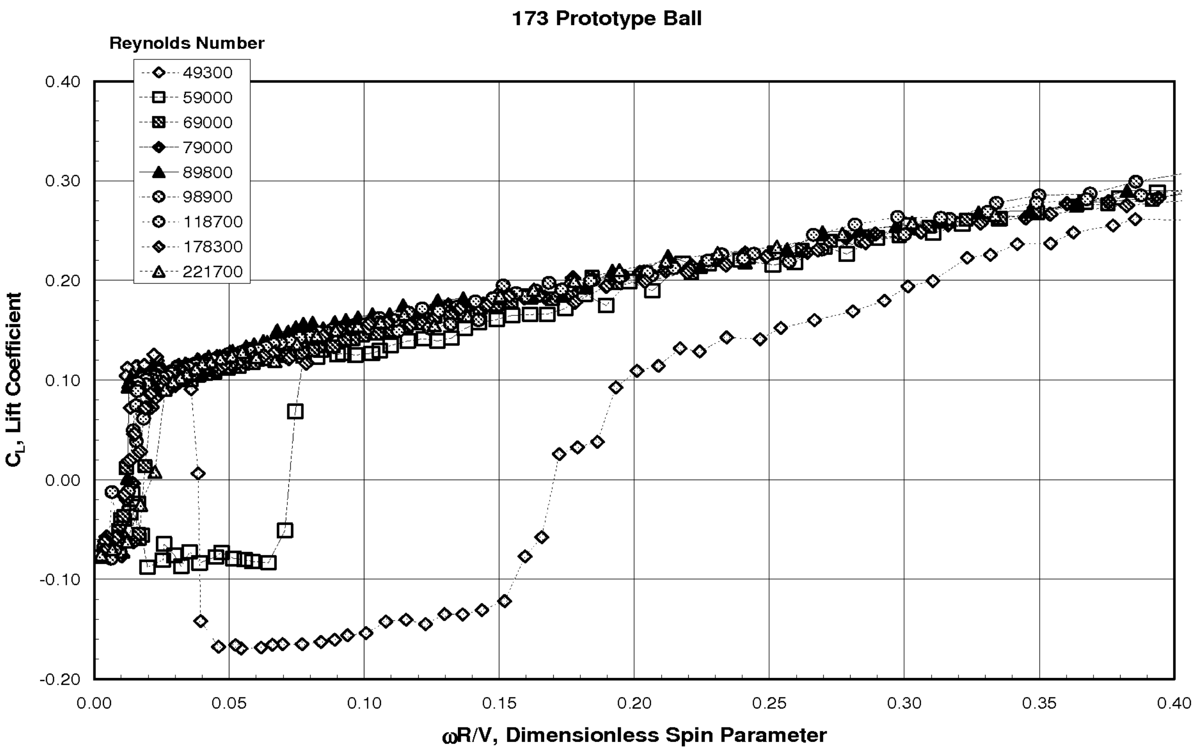
173 Prototype Ball
Reynolds Number
49300
59000
69000
79000
89800
98900
118700
178300
221700
0.40
0.30
0.20
0.10
0.00
-0.10
-0.20
C_L, Lift Coefficient
0.00
0.05
0.10
0.15
0.20
0.25
0.30
0.35
0.40
ωR/V, Dimensionless Spin Parameter

FIG. 17

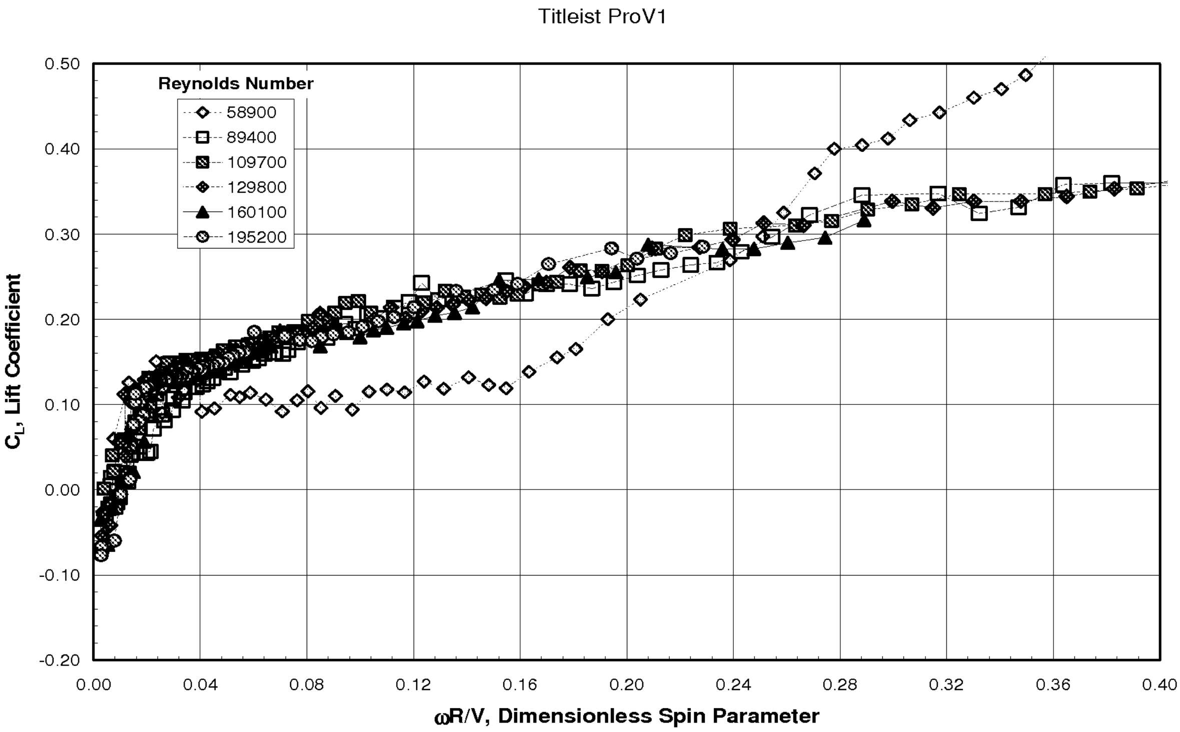
Titleist ProV1
Reynolds Number
58900
89400
109700
129800
160100
195200
C_L, Lift Coefficient
0.50
0.40
0.30
0.20
0.10
0.00
-0.10
-0.20
0.00
0.04
0.08
0.12
0.16
0.20
0.24
0.28
0.32
0.36
0.40
ωR/V, Dimensionless Spin Parameter

FIG. 18

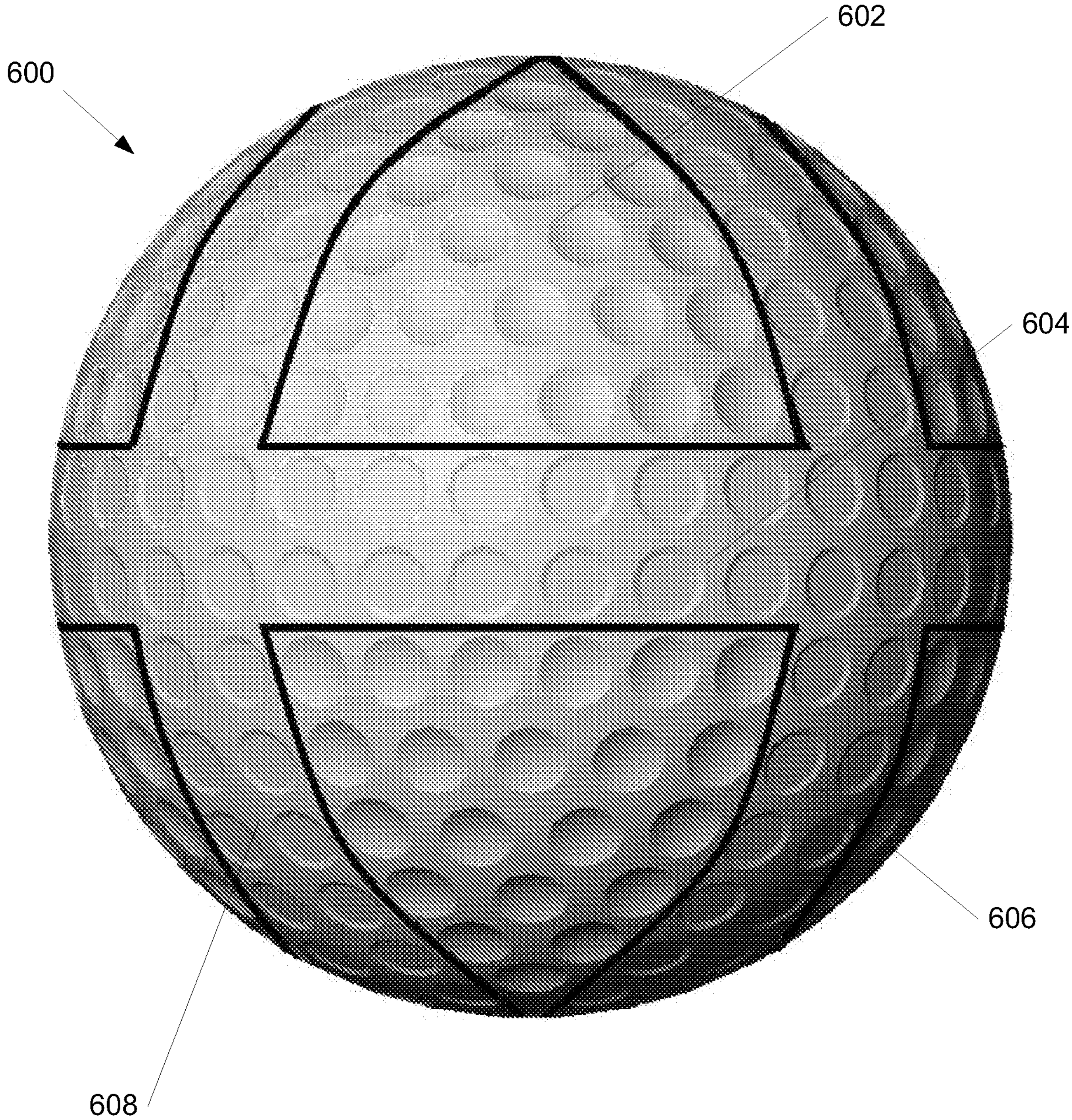

FIG. 19

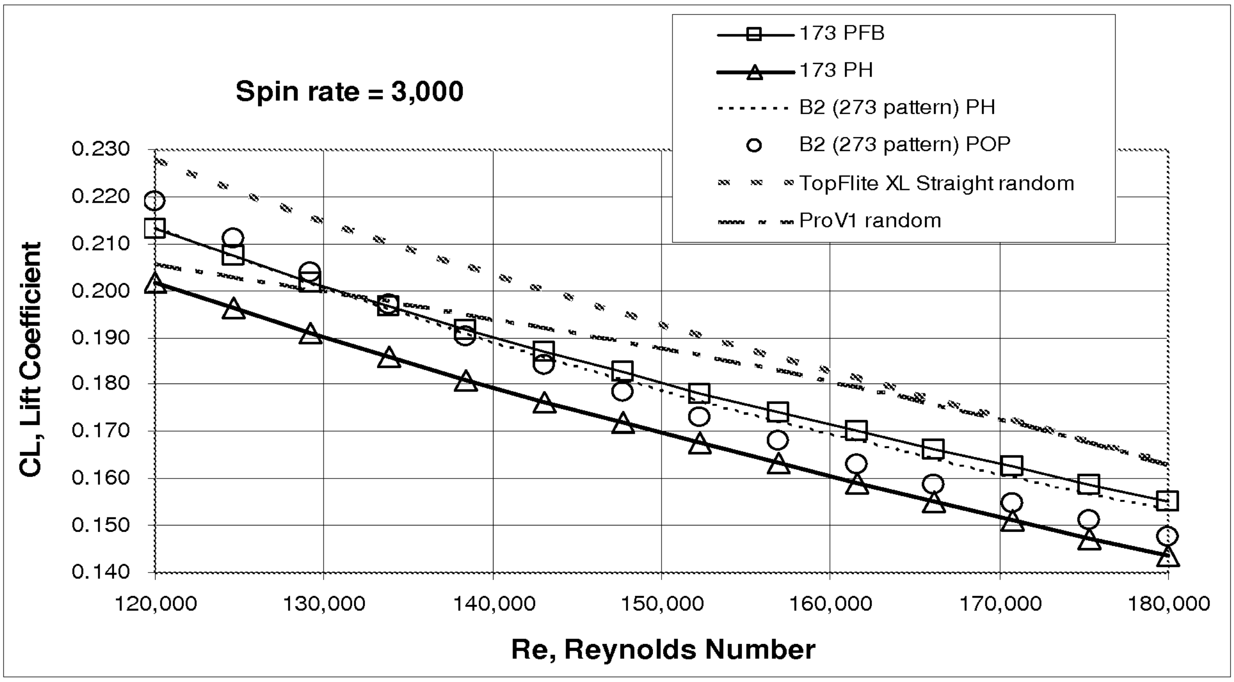
Spin rate = 3,000
173 PFB
173 PH
B2 (273 pattern) PH
B2 (273 pattern) POP
TopFlite XL Straight random
ProV1 random
CL, Lift Coefficient
0.230
0.220
0.210
0.200
0.190
0.180
0.170
0.160
0.150
0.140
120,000
130,000
140,000
150,000
160,000
170,000
180,000
Re, Reynolds Number

FIG. 20

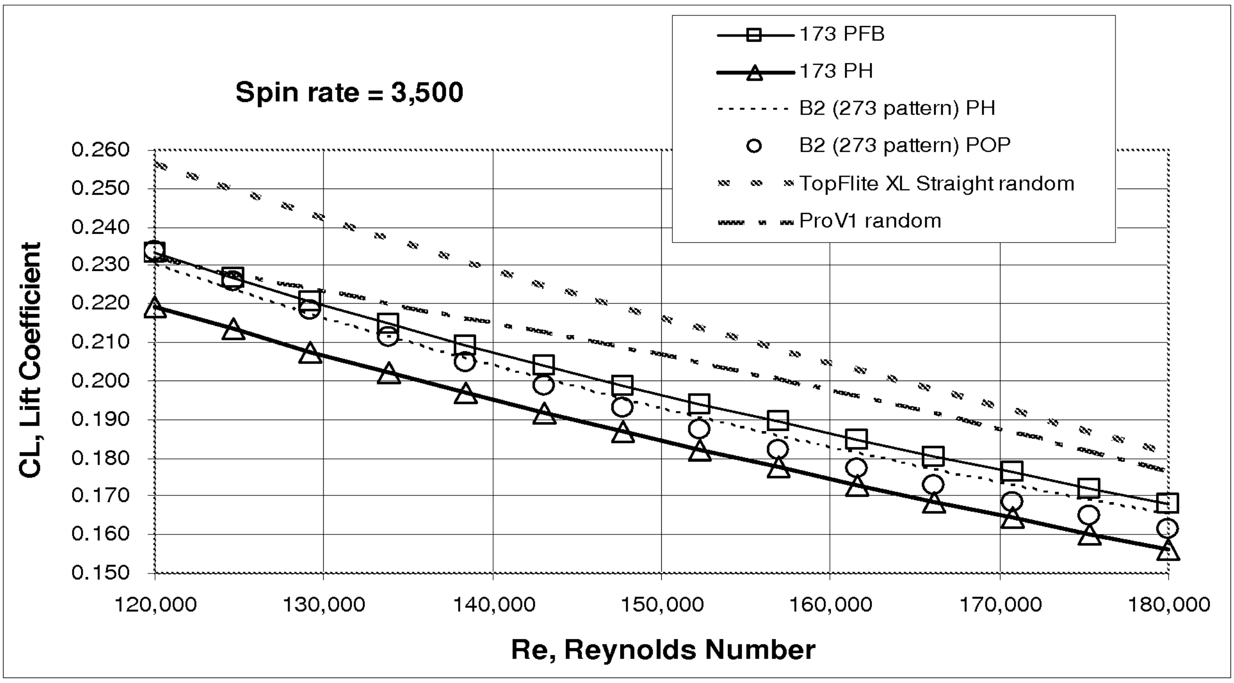

Spin rate = 3,500
173 PFB
173 PH
B2 (273 pattern) PH
B2 (273 pattern) POP
TopFlite XL Straight random
ProV1 random
0.260
0.250
0.240
0.230
0.220
0.210
0.200
0.190
0.180
0.170
0.160
0.150
CL, Lift Coefficient
120,000
130,000
140,000
150,000
160,000
170,000
180,000
Re, Reynolds Number

FIG. 21

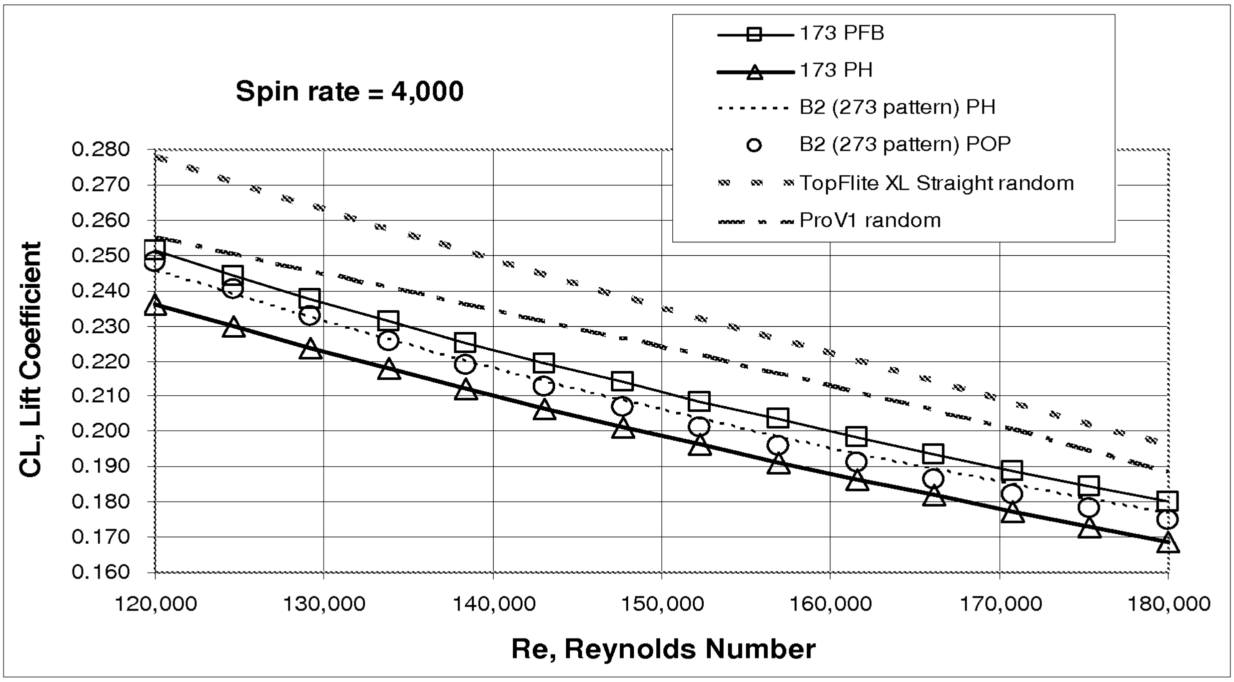
173 PFB
173 PH
B2 (273 pattern) PH
B2 (273 pattern) POP
TopFlite XL Straight random
ProV1 random
Spin rate = 4,000
0.280
0.270
0.260
0.250
0.240
0.230
0.220
0.210
0.200
0.190
0.180
0.170
0.160
CL, Lift Coefficient
120,000
130,000
140,000
150,000
160,000
170,000
180,000
Re, Reynolds Number

FIG. 22

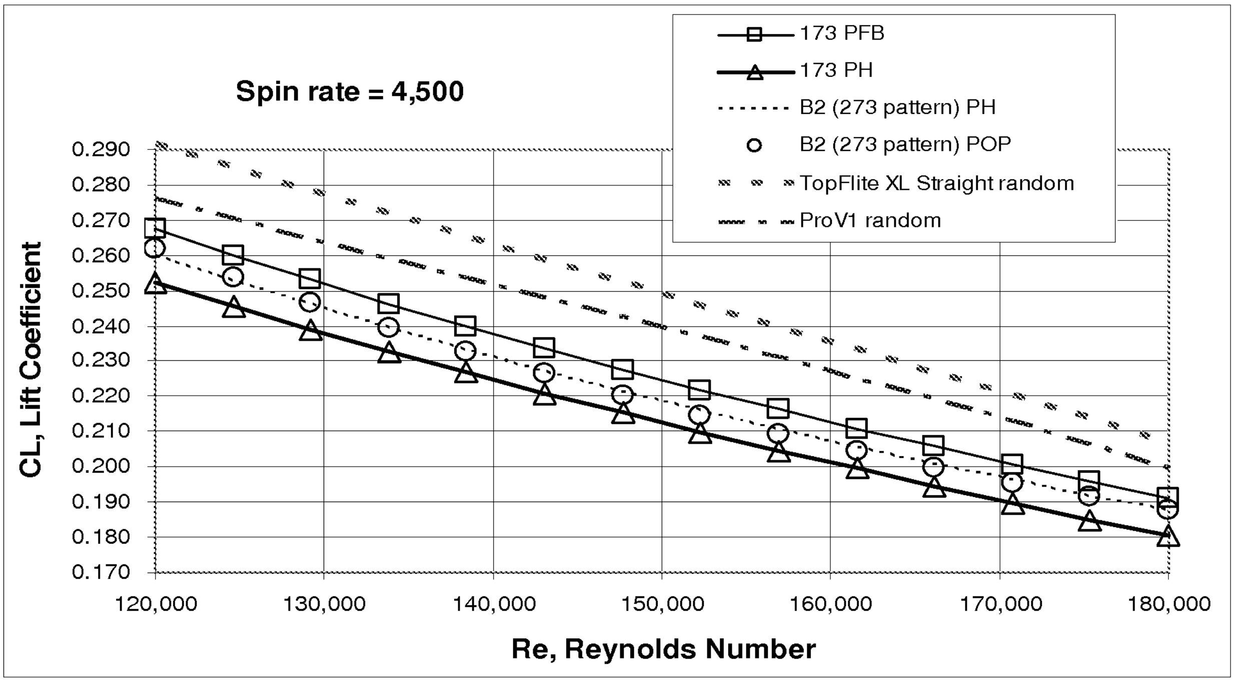
Spin rate = 4,500
173 PFB
173 PH
B2 (273 pattern) PH
B2 (273 pattern) POP
TopFlite XL Straight random
ProV1 random
CL, Lift Coefficient
0.290
0.280
0.270
0.260
0.250
0.240
0.230
0.220
0.210
0.200
0.190
0.180
0.170
120,000
130,000
140,000
150,000
160,000
170,000
180,000
Re, Reynolds Number

FIG. 23

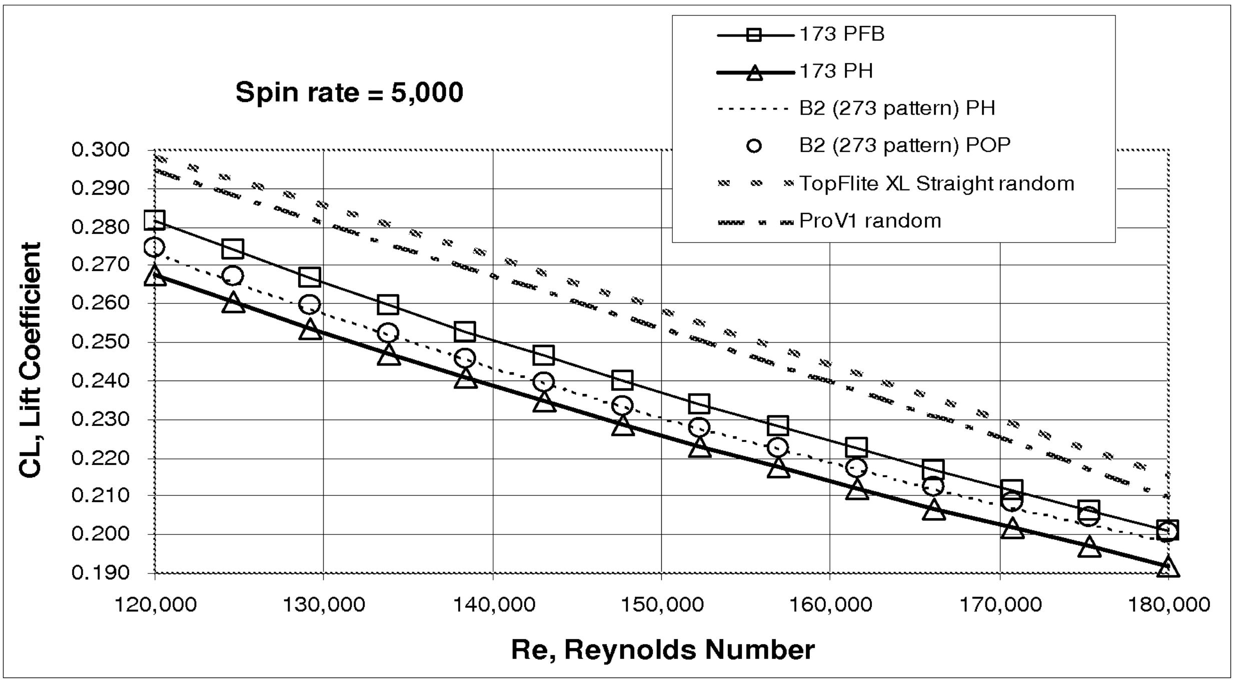
Spin rate = 5,000
173 PFB
173 PH
B2 (273 pattern) PH
B2 (273 pattern) POP
TopFlite XL Straight random
ProV1 random
CL, Lift Coefficient
0.300
0.290
0.280
0.270
0.260
0.250
0.240
0.230
0.220
0.210
0.200
0.190
120,000
130,000
140,000
150,000
160,000
170,000
180,000
Re, Reynolds Number

FIG. 24

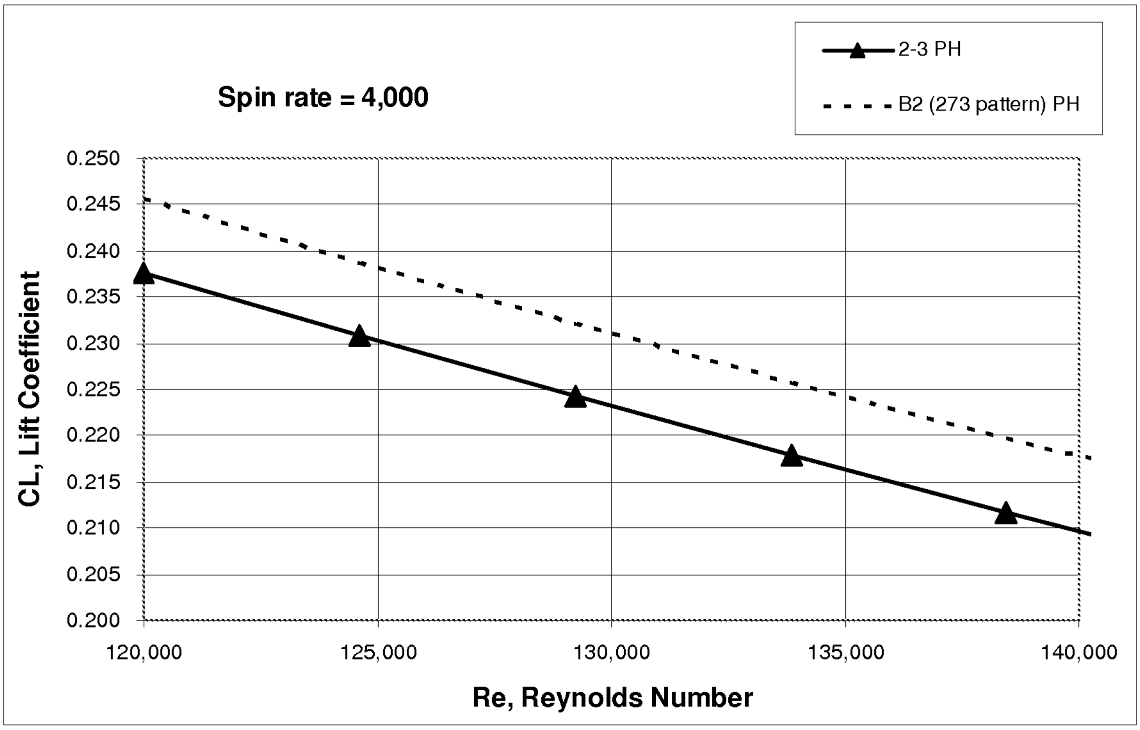
2-3 PH
B2 (273 pattern) PH
Spin rate = 4,000
0.250
0.245
0.240
0.235
0.230
0.225
0.220
0.215
0.210
0.205
0.200
CL, Lift Coefficient
120,000
125,000
130,000
135,000
140,000
Re, Reynolds Number

FIG. 25

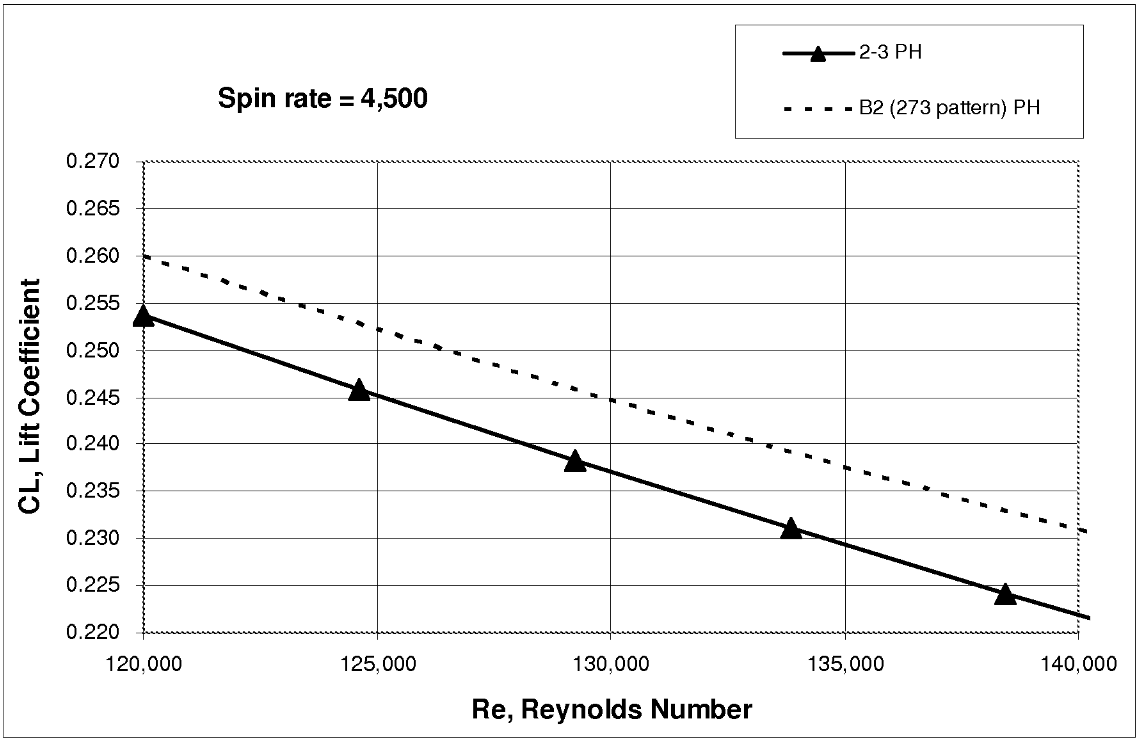
Spin rate = 4,500
2-3 PH
B2 (273 pattern) PH
0.270
0.265
0.260
0.255
0.250
0.245
0.240
0.235
0.230
0.225
0.220
CL, Lift Coefficient
120,000
125,000
130,000
135,000
140,000
Re, Reynolds Number

FIG. 26

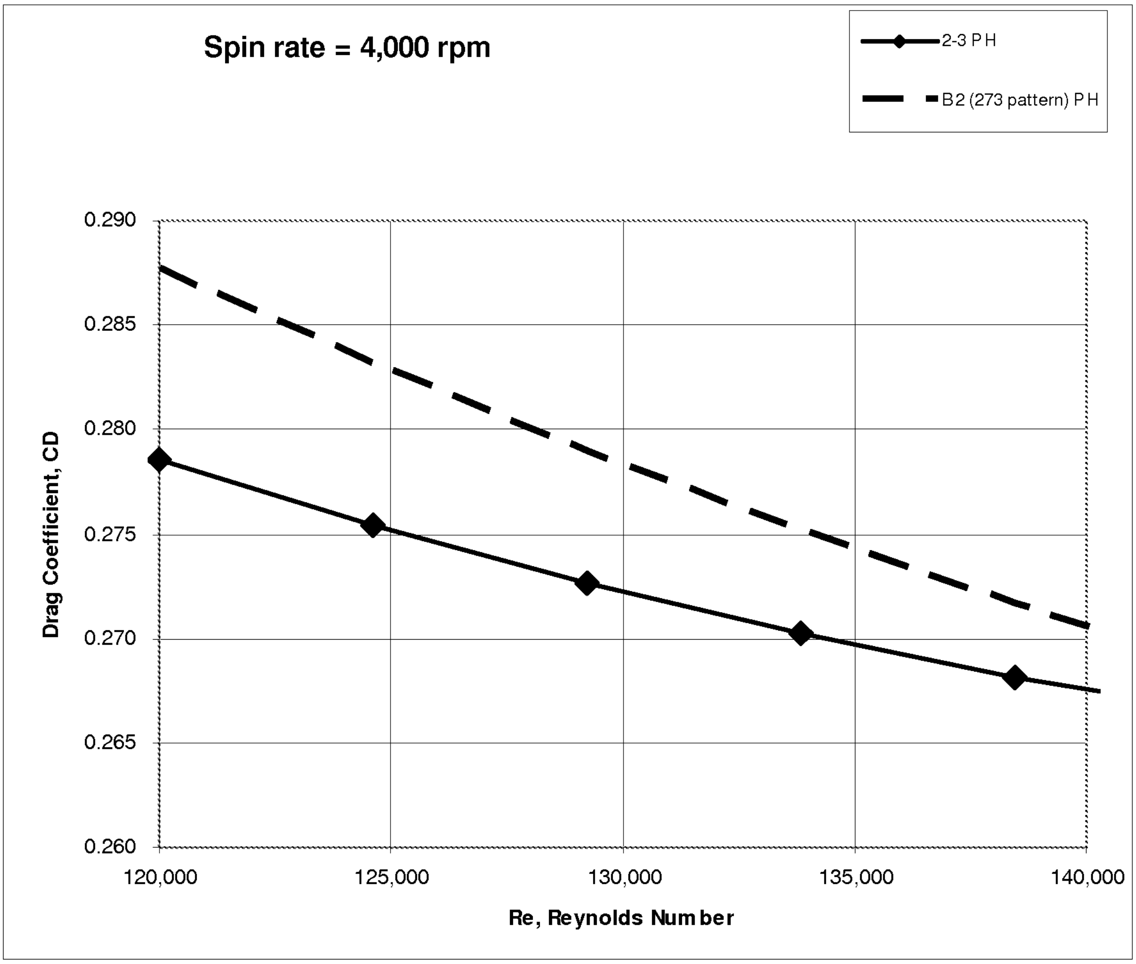
Spin rate = 4,000 rpm
2-3 PH
B2 (273 pattern) PH
0.290
0.285
0.280
0.275
0.270
0.265
0.260
Drag Coefficient, CD
120,000
125,000
130,000
135,000
140,000
Re, Reynolds Number

FIG. 27

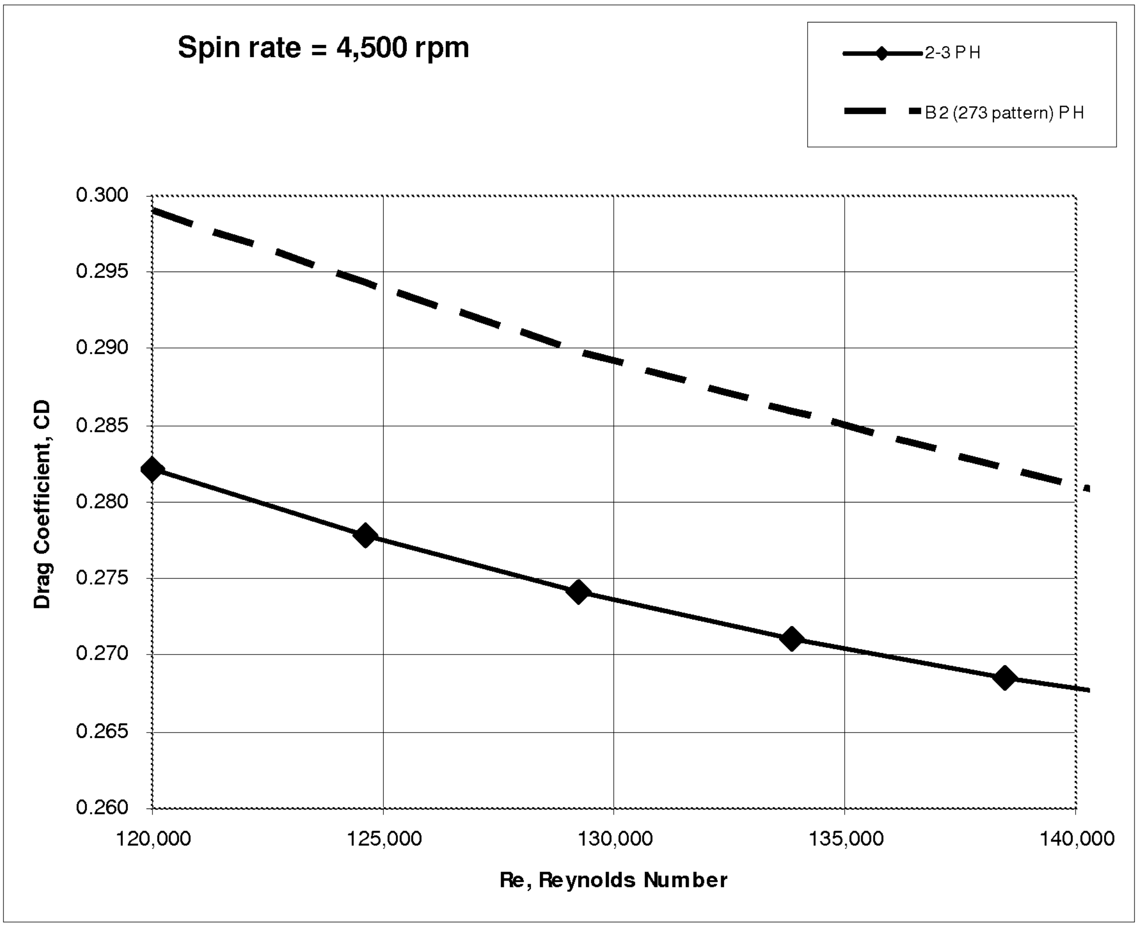
Spin rate = 4,500 rpm
2-3 PH
B2 (273 pattern) PH
0.300
0.295
0.290
0.285
0.280
0.275
0.270
0.265
0.260
Drag Coefficient, CD
120,000
125,000
130,000
135,000
140,000
Re, Reynolds Number

FIG. 28